

Regional Gravity Survey of Silver Spurs Ranch

Wes Wilson

Sangre Geophysics

November 2, 2006

Disclaimer:

Opinions expressed are solely those of the author and do not reflect those of the Silver Spurs Property Owners Association.

Motivation

The geology of the Spanish Peaks area is unique. Emplacement of the Spanish Peaks created a series of radial faults which allowed the formation of dikes that permeate the region.

Many ground water systems are fracture controlled. Dikes and associated fracture patterns create a complex water flow regime where groundwater flow is redirected by impermeable dikes. By understanding large scale fractures and subsurface dike locations, connected regions of water flow can be identified.

The purpose of this study is to establish whether or not the Spanish Peak dikes extend into Silver Spurs Ranch, and if so, where are they and at what depth. Results are evaluated to determine possible connected water flow regions and possible areas of recharge where the water flow is replenished.

A geophysical gravity survey is a relatively inexpensive method for mapping the subsurface of large regional areas. This report presents the results of a regional gravity survey conducted over the Silver Spurs Ranch in June, 2006.

Regional geology

The surface geology of the Spanish Peaks area has been strongly influenced by the formation of the Spanish Peaks. The Spanish Peaks are thought to be large intruded magma bodies called stocks or batholiths. These bodies formed at depth some 27 million years ago and gradually became visible as the softer overlying rock eroded away.

When the Spanish Peak stocks were formed, vertical forces of the hot rock caused fractures to form in the overlying sedimentary rocks. As the fractures were created, hot magma flowed into the cracks to form the dikes. Figure 1 shows an outcrop of a typical dike just north of the town of La Veta. Typical widths of the dikes range from a few meters to tens of meters.

Simple mathematical models based on point stresses in thin plates predict the expected fracture pattern for such an emplacement to be radial arcs. These arcs curve at the ends to align with existing horizontal stress in the plate. Figure 2 shows the Spanish Peaks as seen from a point of view above Silver Spurs Ranch looking west. Major dikes are outlined in blue to emphasize their radial nature. Not all dikes follow the same radial pattern. This suggests that the dikes most likely formed over a period time under different stress conditions.

Horizontal and vertical stresses associated with the dikes also left an imprint of vertical faults in the weaker overlying sedimentary layers. Figure 3 shows vertical fractures in the Trinidad sandstone formation, a rock layer found beneath Silver Spurs Ranch.

Dikes and vertical fracturing control water flow through out the region. The ability of water to flow through rock is measured as permeability. Permeability of the dike rock is higher than the surrounding sedimentary rock. When water flow encounters a buried dike, it is diverted along the vertical plane of the dike. Water flowing in sedimentary rocks will seek out channels provided by existing vertical fractures. The combination of dikes and fractures creates a complex water flow pattern in the region. By understanding the location of the dikes both above and below the surface, water barriers created by dikes can be outlined to understand water flow patterns.

The physical properties of the dike rock that create higher permeability also make the rock heavier or denser. Surrounding sedimentary rock is less dense than the dike rock. A gravity survey takes advantage of the density contrast to map the location of the subsurface dikes.

Gravity survey design

A gravity survey measures the pull of gravity at various survey locations. The pull of gravity varies as a function of rock density. Gravity differences on the surface of the earth are small but measurable. Refer to Appendix C for a detailed description of the gravity exploration method as presented by the United States Geological Survey (USGS).

A gravity survey is one of the most inexpensive geophysical techniques for mapping the subsurface. The survey is conducted by taking a series of measurements over the survey area. A regional gravity survey was conducted on Silver Spurs Ranch over the period June 16 - 20, 2006. Gravity measurements were taken along existing roads at a spacing of 100 meters (m). This resulted in 368 measurements along 36.8 linear kilometers (23 miles). The survey covered approximately 31 square kilometers (12 square miles). Measurement locations are shown with respect to the Spanish Peaks in Figure 4.

To determine density contrast, rock samples were taken from several locations on Silver Spurs Ranch (The Ranch). Densities for rock sample locations shown in Figure 4 are listed in Table 1. Samples WAL1 and WAL2 are taken from a dike outcrop along Highway 85 north of Walsenburg. They indicate an average dike density of 3.85 grams per cubic centimeter (g/cc).

| site | rock type | density g/cc |
|------|------------|-----------------|
| WAL1 | hornblende | 4.09 |
| WAL2 | hornblende | 3.60 |
| SSP1 | sandstone | 2.36 |
| SSP2 | sandstone | 2.37 |
| SSP3 | sandstone | 2.63 |
| SSP4 | sandstone | 2.37 |

Table 1 Rock sample density measurements.

The average density of the 4 sandstone samples is 2.43 g/cc. A density difference of 1.42 g/cc between the sandstone and dike rocks is large enough to create a change in gravity that can be measured by an exploration gravity meter.

Gravity surface locations are displayed on a USGS topographical map in Figure 5. Universal Transversal Mercator (UTM) coordinates are annotated along the map axes. Gravity station (stn) locations and the corresponding UTM coordinates (XYs) are listed in Appendix B.

Roads on the USGS maps are taken from an older vintage aerial photo and the road locations vary from their present day locations as shown by gravity survey markers along current roads. For reference, the property map, Figure 6, will be shown with the gravity maps. The property map is shown with a digital elevation map in Figure 7.

Gravity measurement

At each survey location a gravity measurement is made along with latitude, longitude and elevation. Layout for a typical gravity measurement is shown in Figure 8. The gravity meter is about the size of a car battery and is shown with the aluminum carrying case. The carrying case contains a battery which powers the temperature control and readout displays. The top view of the gravity meter shows the controls, Figure 9. A measurement is made by first setting the meter on a tripod

base. The instrument is leveled using the large knobs on the left side corners and middle right. Once level, the aluminum dial is rotated until the 'beam' galvanometer in the upper right reads zero or is straight up. Gravity values are then read off the aluminum dial.

Once the gravity value is read, the latitude, longitude and elevation are read from the Garmin GPS receiver shown at the upper left in Figure 8. The latitude/longitude GPS coordinates were read to within an accuracy of about 10-20 meters. Vertical measurements of elevation were accurate to 20m at best. For a gravity survey, accurate vertical elevation measurements are critical for determining gravity corrections. To improve vertical accuracy, the latitude/longitude locations for each measurement were used to locate the corresponding elevation on the USGS map in Figure 5. The Garmin GPS receiver and the USGS map use the WGS84 projection. Elevations (elev) in meters for each location are listed in Appendix B.

Measurements are noted in the black survey book, the meter is locked and set into the aluminum carrying case, equipment is loaded into the truck and the next survey location is found by driving along the road 100m using the GPS receiver for reference. Each measurement took from 4-8 minutes.

A cross section of the gravity meter is shown in Figure 10. The gravity meter contains a sensitive spring which balances an internal mass on a beam. The mass is balanced by turning the nulling dial which corresponds with the aluminum dial shown in Figure 9. The gravity meter used for the survey was a Lacoste and Romberg D meter with a sensitivity of about .1 mgal gravity units. For reference, the surface gravity along the equator of the earth is about 1 million mgal. The gravity meter measures to less than 1 part per million of the total gravity field.

Gravity corrections

A number of factors influence a gravity measurement. When the gravity survey is corrected for known variations, the resulting gravity map shows the unknown or anomalous gravity. Gravity anomalies are modeled mathematically based on known density variations to determine possible subsurface bodies or, in this case, dike locations.

Gravity measurements are affected by the following known factors:

- Electronic instrument drift during the course of the survey
- Tidal variation caused by the sun and moon
- Latitude variations caused by the shape of the earth
- Elevation differences along the survey profile
- Density difference beneath a corrected datum elevation
- Elevation differences in the surrounding terrain

Electronic instrument drift occurs in any electronic instrument. Instrument heating, stray capacitance and other factors cause a measuring device to change slightly over time. The gravity meter is no exception. To correct for instrument drift, base stations are established during the survey as reference points. A base station measurement is made, several gravity station measurements are made and then the base station is re-measured to identify any instrument drift. For this survey, a base station was re-measured every 2 hours at a maximum. Instrument drift is assumed to be linear between stations and is removed from the measurements. Details of each correction are summarized in Appendix A.

Tidal pull of the sun and moon also affect the gravity measurement. Tidal corrections can be computed mathematically, but in general the variation is assumed to be linear over the time frame of the drift correction. The correction is applied at the same time as the drift correction. Appendix B shows the actual field reading from the gravity meter, 'field g', in gravity meter units. The 'rel g' column shows the relative gravity value in mgal units with the drift corrections applied. The survey

base station was established on the SE corner of the driveway at 463 Leather Dr. To find absolute gravity measurements the 'rel g' value is added to a known gravity station established by the US Geodetic Survey. Such a station exists at Trinidad Junior College and a measurement was made for completeness of the survey. However, when looking for anomalies, only the change in gravity is needed. Therefore, relative gravity changes are used for interpretation.

Gravity is caused by presence of mass. Any object with mass has a gravitational attraction. As one moves away from the mass, the gravitational attraction decreases. The same is true for the earth. As one moves away from the earth, the gravitational attraction decreases. The earth is not completely solid and as the earth turns, the centrifugal force causes the earth to bulge along the equator. The bulge causes the surface of the earth to be farther away from the center of the earth at the equator than at the poles. This causes the measured gravity to be lower at the equator than at the poles. The change is a function of the shape of the earth, and the shape is well known from satellite measurements. The correction is known as a latitude correction formally defined as the International Association of Geodesy Reference System 1980. Gravity measurements with the applied latitude correction are listed in the column marked 'latitude' in Appendix B.

Elevation change causes a change in gravity. An elevation profile along Silver Spurs Rd from north to south, Figure 11, shows an elevation variation of approximately 170m. For an average density of 2.67 g/cc, this elevation difference results in a gravity change of 50 mgals. Since the dike anomalies are less than 10 mgals, an elevation correction must be made to the field measurements. The correction is called a free air correction. The 'free air' column in Appendix B shows the gravity measurements which have been corrected for drift, latitude and elevation. These measurements are referenced to a constant elevation datum of 2076 m, the elevation of the base station.

The free air gravity values are contoured to generate a free air anomaly map, Figure 13. The anomaly map is shown with the digital elevation map in Figure 12. Color contours are in gravity units of mgal shown annotated on the color bar. The free air anomaly map generally follows the topography. Figure 12 shows gravity highs in red roughly following the elevation highs along the ridges found on The Ranch.

Two additional corrections are necessary before attempting an interpretation, the Bouguer correction and the terrain correction. The free air correction compensates for elevation variations with reference to a datum elevation. The Bouguer correction adjusts the gravity measurements to fill in the surface below the datum and removes the surface above the datum. The resulting gravity measurement is as if it was measured on a flat surface at the datum elevation. The Bouguer correction is combined with the free air correction to generate the 'bouguer' values in Appendix B. The corresponding Bouguer anomaly map is seen in Figures 14 and 15.

The Bouguer anomaly map highlights regions of excess mass. A large positive anomaly of 3 mgal is seen around properties 39 and 40 along Silver Spur Rd. Although large, it is smaller than the free air anomaly of 11 mgals at the same location. There does not appear to be a direct correlation of the anomalies with the topography. This suggests that a gravity correction related to the surrounding terrain may be necessary.

The complete Bouguer anomaly maps, Figures 16 and 17, take into account terrain corrections about each gravity measurement. Appendix B lists the anomaly values in the column marked 'complete.' The complete Bouguer anomaly map shows a general correlation with topography as expected and will form the basis of the gravity interpretation.

Gravity modeling

The complete Bouguer anomaly map shows remaining gravity variations after all corrections are made. Anomalies associated with the near subsurface geology are interpreted by matching a

computed gravity field above blocky models to the observed gravity anomaly. When the field matches, one possible solution has been determined. The technique is referred to interchangeably as either 'modeling' or 'interpretation.'

The gravity field for simple geometric structures like rectangles and n-sided polygons can be computed for a given density. To simplify the gravity modeling, the subsurface can be assumed to be 2 dimensional (2D). This assumption gives a good approximation when the 2D cross section is taken perpendicular to the trend of the gravity anomaly. A 3D approximation is made by assuming that the 2D model continues into and out of the plane. This is called a 2.5D approximation. To visualize, one can consider a loaf of bread. The slice of bread in the center of the loaf would be the 2D model and the entire loaf of bread would be the 2.5D model.

Gravity modeling was accomplished with Geomodel, a modeling software package. The program allows a user to interactively define 2.5D geometric blocks to match the observed gravity anomaly. Block vertices can be adjusted interactively to refine the interpretation.

The complete Bouguer anomaly map with 6 selected 2.5D profiles lines is shown in Figure 18. Four of the lines are taken along the trend of the gravity anomalies and two are taken perpendicular. Gravity values are extracted along these profiles and block models are created to match the gravity changes.

Profile AA', Figure 19, is a 2D cross section which starts near the end of Rope Ct and trends northeast to Reins Rd. The starred (*) points represent gravity values in mgals which have been extracted from the complete Bouguer map along the AA' profile. The solid line is the gravity computed for the model blocks shown in green. Depth and horizontal axis units are meters.

The object of gravity modeling is to match the computed gravity anomaly with the observed gravity values. The resulting model reflects the depth and extent of dike structures.

A constant density is required for computing the gravity field. Values shown on the green blocks represent density contrast values between the dike rock and the surrounding sandstone. Referring to Table 1 for measured density values, a value of 1.5 was chosen to represent the density contrast. This value was used for all density blocks for consistency. Surface positions and lateral extent of the density blocks are shown in Figure 25.

The topographic map, Figure 16, suggests that ridges to the west of the survey may extend into the The Ranch. Body 1 on Profile AA' indicates a dike extending along the trend of the ridge possibly extending the length of Profile AA'. Body 2 is a cross cutting dike. It shows up again in Profile BB' and extends the length of Rowell Rd to Sunset Ct. Body 3 required a long lateral extent to match the gravity anomaly. The lateral extent may indicate a possible influence from the large gravity anomaly related to Body 4. A dike outcrop in the creek bed along Silver Spur Rd indicates that the dike associated with Body 3 most likely trends to the northwest. Body 4 has a large associated gravity anomaly and may either be an extension of the dike from the south or an extension from a dike trending west to east outside The Ranch or both. Depths to the top of the dikes vary from 80-90m for dikes 1 and 2 along the south side to depths of 140-200m along Reins Rd to the north. Figure 26 shows a possible interpretation of the cross cutting dike structure.

Profile BB', Figure 20, starts along Silver Spur Rd to the north and runs SSE to the south end of The Ranch. As mentioned, Body 1 most likely extends along Rowell Rd to Sunset Ct and possibly beyond. Body 2 is a broad gravity anomaly that ranges across The Ranch to at least Sunrise Rd. A short lateral extent was used for the density block. The computed gravity anomaly was relatively insensitive to lateral extent because of the required depth of the perturbing blocks. The dike appears to start around Boot Ct and extends to Sunrise Rd. Body 3 indicates a cross cutting dike structure that trends west to east along Horseshoe Ct and Leather Dr. The anomaly is discussed in detail for Profile EE'. Similarly, Body 4 shows the intersection of Profile BB' with the Small Dike anomaly along Profile FF'. Depths to top of the anomalies range from 110-140m for the narrow

cross cutting dikes, Bodies 3 and 4, to a relatively deep 325m for the broad anomaly associated with Body 2.

Profile CC', Figure 21, follows Sunrise Rd and intersects Small Dike to the south. Body 1 may be a small dike following the west to east trend shared with the major dike features. Body 2 is an extension of the broad gravity anomaly seen along Profile BB'. The gravity anomaly appears smeared and may indicate 3D effects from nearby features. Profile DD' along the ridge of the broad dike feature shows a break in the anomaly at the intersection with Profile BB'. The break may indicate a fault which strikes NNE and will be discussed in more detail when profiles DD' and EE' are evaluated. Body 3 represents the intersection with Small Dike to the south. Bodies 1 and 3 are at depths of 200 m and 180 m respectively. Body 2 is modeled at a depth of 300 m and may reflect a discontinuity along the west to east anomaly modeled in Profile DD'.

Profile DD', Figure 22, starts on the west at Boot Ct, traverses across Silver Spur Rd to Sunrise Rd and ends along Trails End Dr to the east. The gravity anomaly is wide and may indicate a contribution from a second dike within the anomaly. A single polygon is used to model the gravity anomaly since the profile traverses along the ridge of the anomaly. The anomaly begins abruptly around the start of Boot Ct. Profile DD' shows the top of dike gently dipping to the east, starting at a depth of 315m and dropping to a depth of 1700m. A small anomaly along Rodeo Dr brings the depth back to 30m near the surface. The depth plunges to 4000m and then returns to 250m beneath Trails End Dr. The large depth variation may indicate the dike is offset by a fault. Further evidence for a fault can be found along Profile EE'. The interpretation of the dike and fault are shown in Figure 26.

Profile EE', Figure 23, starts along Horseshoe Circle to the west and travels along Leather Dr down to the old Hezron Mine. The top of the interpreted dike varies from 200-300m along the profile until about property 107 where the interpreted dike drops to a depth of 2000m then returns to a depth of 400m along the Hezron mine ridge. The drop along the top of the surface of the model is interpreted as a fault in Figure 26.

Profile FF', Figure 24, starts along Green Horn View Lane, travels along Silver Spur Rd following Small Dike and ends along Cherokee Lane to the east. The top of the model drops to a depth of 1500m where it first intersects Silver Spur Rd. This may indicate a fault or a smaller cross cutting dike feature. The model returns to a depth of 140m before dropping again to 1500m. This second drop is interpreted as an extension of the fault along Sunrise Rd and Leather Drive. The model returns to a depth of 220m along Cherokee Lane.

Profiles BB' and CC' extend into what appears to be a broad, isolated basin between Small Dike and Big Dike on the south end of The Ranch. A small gravity high occurs in the basin around property 134, but the basin is featureless for the most part. Small gravity changes do not necessarily translate into small topography changes. A surface elevation change of 70m along Pryor Canyon is seen in the same area.

Water Regions

Dikes form impermeable boundaries to water flow. Knowing the position of the dikes, possible water flow regions can be inferred. Figure 27 shows five possible recharge regions associated with the interpreted dike positions. Recharge areas are marked with blue arrows. Any changes to recharge regions in the blue arrow areas may impact well performance in the associated regions on The Ranch.

Region I in the northwest corner of The Ranch was not included in the gravity survey but from the topographic expression of dikes to the west, it is reasonable to assume that water recharge occurs along the dike to the immediate south and is replenished with any available water resource coming from the northwest. The recharge area is marked with blue arrow 1.

Region II at the north end of the Ranch receives recharge water from the south side of the dike to the immediate west. The recharge area is marked with blue arrow 2. The interpreted dike along Reins Rd may redirect the recharge coming from the west causing shadow zones on the east side of the dike. An alternate recharge region to the northeast is marked with blue arrow 4.

Region III in the center of The Ranch has a possible recharge area occurring along Walsen Creek. The digital elevation map, Figure 27, shows a large fault offsetting Big Dike along Walsen Creek as indicated with blue arrow 3. The fault offset creates a gap of 100m allowing water recharge to flow off the slopes of East Spanish Peak and enter the Region III water regime from the south. The interpreted dike which begins along Chaps Ct and extends along Rowell Rd to Sunrise Ct may discourage recharge from entering Region II from this recharge source. Small Dike bounds Region III on the south. Seasonal recharge occurs along the flanks of Small Dike. Along the northeast margin of Region III recharge marked as blue arrow 4 may occur from the plains to the northeast.

Region IV at the south end of The Ranch is isolated from the other recharge zones by Small Dike and Big Dike. The gravity survey indicates that the region is an isolated basin. Figure 5 shows Pryor Canyon beginning along the west edge of Small Dike. Surface runoff travels down Pryor Canyon seeping into fractures along the surface and recharging water resources at depth. A similar type of recharge mechanism occurs along the north side of Big Dike. Water recharge marked as blue arrow 5 may also occur on the southeast margin.

Depths to the top of dike structures are greater than 100m in most areas on The Ranch. This means deep water flow is influenced by dike positions, but near the surface water flow is controlled by existing fractures. Figure 3 shows vertical fractures occurring in the Trinidad sandstone. Similar fractures most likely exist in the Raton sandstone that covers most of The Ranch.

Summary

Gravity surveys are a relatively inexpensive geophysical method which can be used to infer simple subsurface features. The intruded dike complex which permeates Silver Spur Ranch provides a density contrast signature which is measurable. The impermeable dikes impact water flow in the region. By knowing the location of subsurface dikes, possible water flow regions are inferred.

The final interpretation, Figure 26, shows dike and fault positions interpreted from the gravity survey. Long linear ridges to the west are consistent with interpreted dikes on The Ranch. Dike ridges tend to lose their distinct appearance once they cross Walsen Arroyo into the Ranch. The gravity survey confirms that the dikes extend into The Ranch at depth.

The gravity anomaly along Reins Rd may represent an extension of a dike from the south west. A dike outcrop in Walsen Arroyo supports this interpretation. The small SSW to NNE trending anomaly which starts at Chaps Ct, crosses Cantrell Rd and continues along Reins Rd, does not correlate well with the predominate dike orientations in the area. However, a dike outcrop along Silver Spur Rd is consistent with the interpretation.

Southwest to northeast trending gravity anomalies correlate well with dikes to the west. Big Dike and Small Dike show positive gravity anomalies. There are 3 smaller east-west trends which indicate buried dikes with depths that range from a hundred meters to thousands of meters.

Along Sunrise Rd the interpreted east-west dike structures drops thousands of meters. This is interpreted as a possible fault which offsets the dike. A large drop in interpreted depth to the top of the structure along Leather Dr and Silver Spurs Rd to south may be an extension of the same fault.

The region south of Small Dike and north of Big Dike on the south end of The Ranch is relatively free of gravity anomalies. This indicates a large basin with water recharge coming from the bounding Big Dike and Small Dike ridges.

Water regions are defined based on dike locations, Figure 27. There are at least four separate water regions with corresponding recharge areas. Dikes permeate the subsurface at depths of more than 100m. This means the dikes control water flow at depth, but near the surface water is controlled by fractures in the overburden.

Future Studies

The gravity survey successfully delineated the general structure of the subsurface dikes. These dikes are a controlling influence on water flow at depth. Above the dikes, water flow is controlled by fractures in the sedimentary rock. Fractures most likely follow the vertical fracture patterns created during the emplacement of the dikes.

For water wells, it is important to know if and where there are fluid filled fractures. One geophysical method that is sensitive to vertical water filled fractures is a method called resistivity. Resistivity surveys measure the electrical conductivity of the earth. A small electrical current is applied to the earth through a pair of electrodes. Another pair of electrodes is used to measure the variation in the electrical field away from the source electrodes. The small current created by 4 D size batteries is non-destructive and does not harm vegetation or structures. A useful study would be to determine the sensitivity of this type of survey in the area.

A near surface seismic survey is more expensive but gives more detail about near surface layers and fracturing. Seismic surveys use a shotgun source which is shot into the ground to generate sound waves. Sound waves are reflected at rock layer boundaries or faults and return to the surface. An array of accelerometers is set on the surface of the earth to record the returning sound waves. Records are processed to create seismic sections which show rock interfaces at depth. The sections outline in detail the existing fracture patterns, but do not guarantee water filled fractures.

Finally, the most accurate measure of the subsurface comes from well data. This is the only direct measurements of the subsurface. Well monitoring will establish seasonal norms for existing wells. A sharp drop or increase from the norm indicates a change in water recharge patterns or water supply. A useful study would be to establish monitoring wells which can be measured monthly. To give a good measurement of static water levels, the monitor well should not be one that is currently being pumped.



Figure 1 Radial dike outcrop along Highway of Legends north of La Veta.



Figure 2 Aerial photo of Spanish Peaks looking west from Silver Spurs Ranch. Major radial dike locations are outlined in blue.



Figure 3 Vertical fractures in the Trinidad sandstone found along County Rd 330 between The Ranch and Walsenburg.

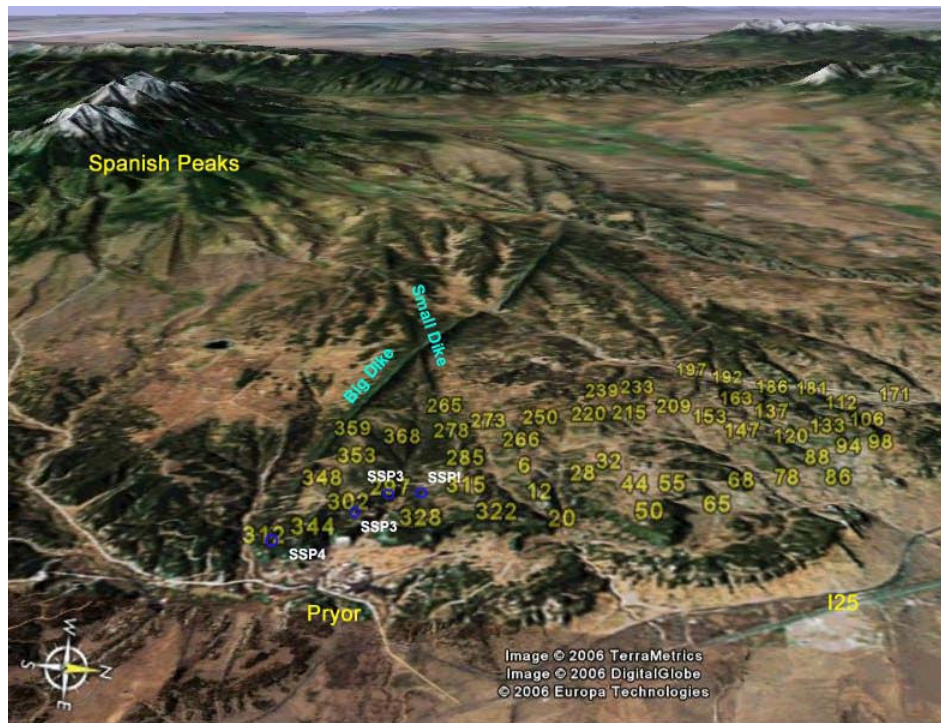


Figure 4 Gravity station locations in yellow and rock sample locations in white. Big Dike and Small Dike can be seen extending into The Ranch.

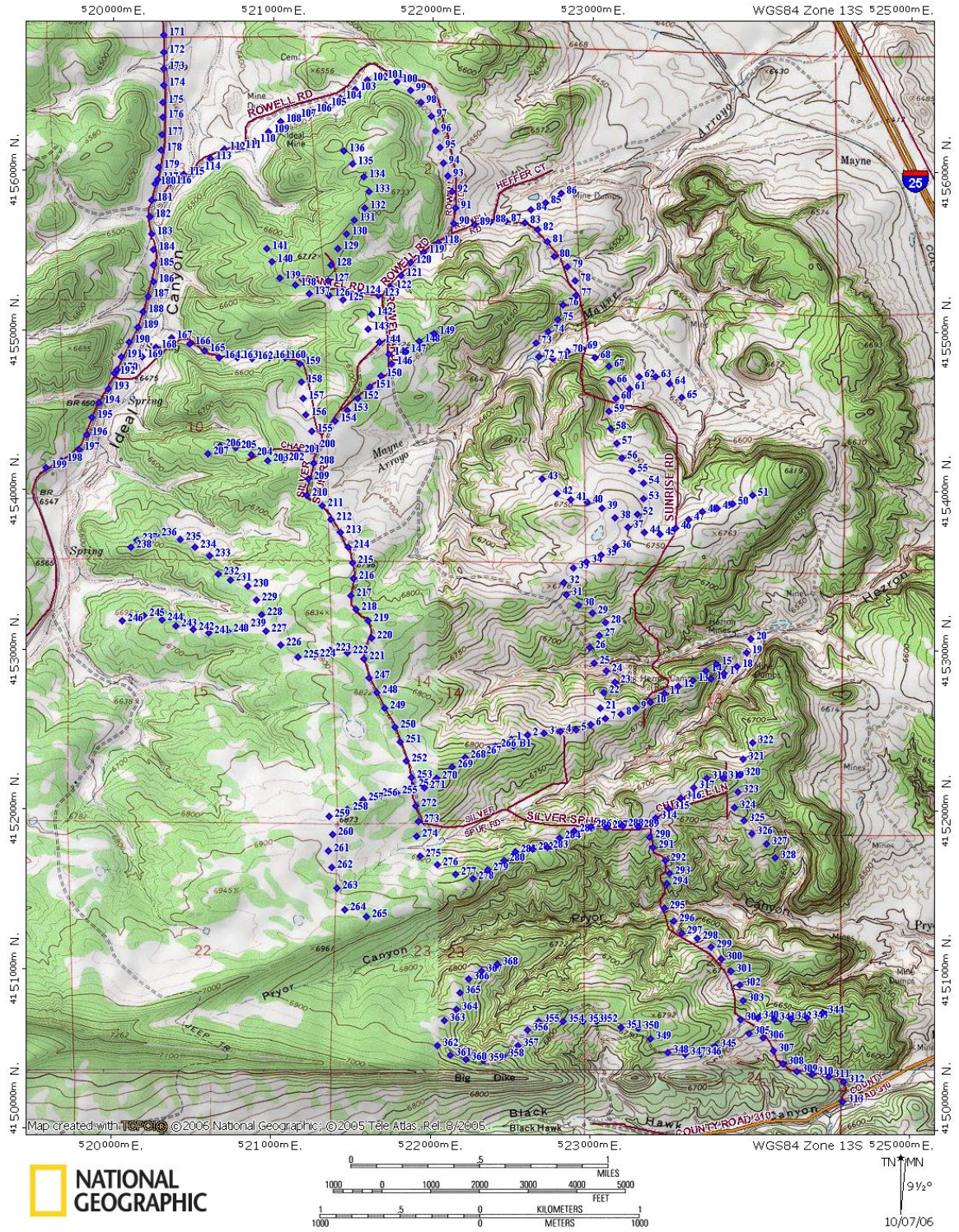


Figure 5 USGS topographic map showing gravity station locations in blue. Road locations appear as they were in the early '90s. Gravity station locations indicate position of current roads.

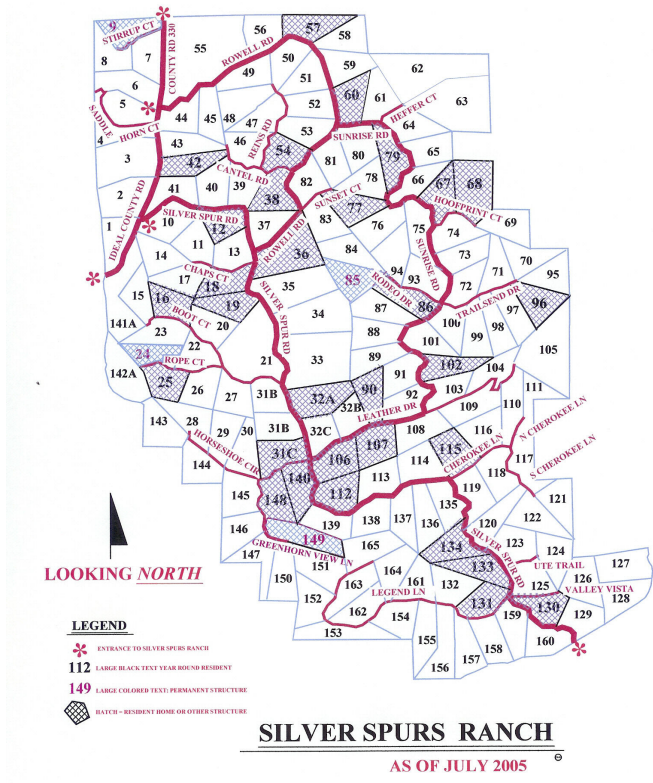


Figure 6 Silver Spurs Ranch property map as of July 2005. The map is used for reference on the gravity anomaly maps.

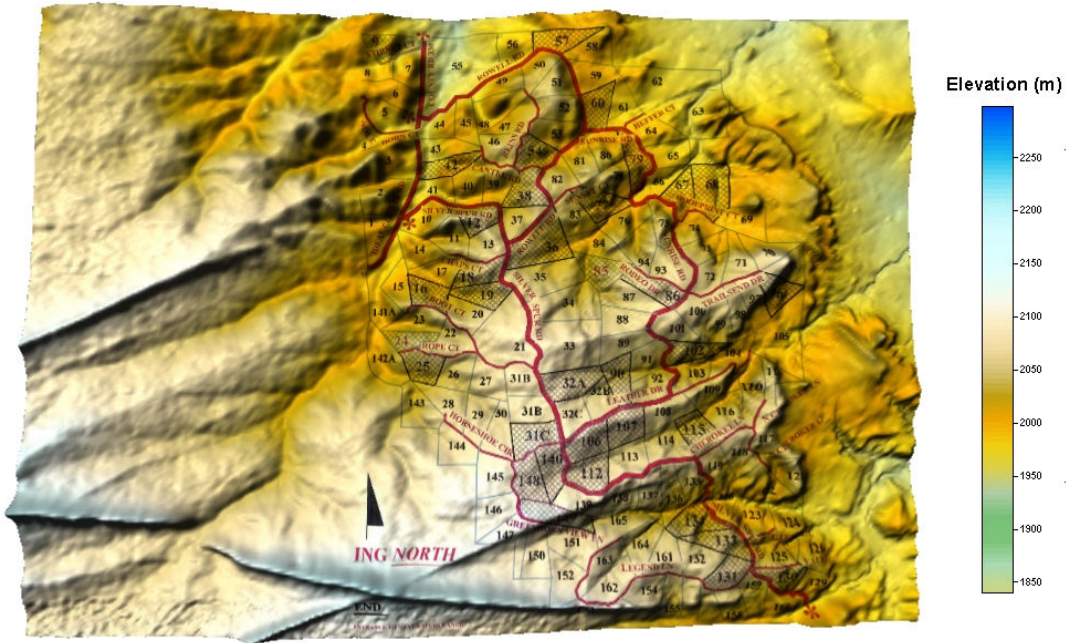


Figure 7 Mosaic of digital elevation maps for the area with property map.



Figure 8 Typical gravity station measurement showing the gravity meter, GPS receiver and field notebook. The towel is for an old man's knees.



Figure 9 Top view of LaCoste and Romberg D gravity meter. Tilt adjustment knobs are located on the left and middle right. Galvanometer dial is above the eyepiece and the aluminum read out dial is in the middle.

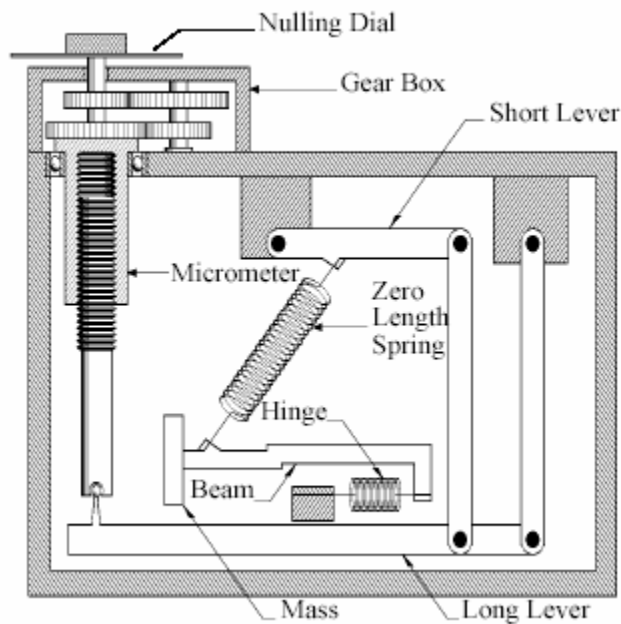


Figure 10 Schematic showing a cross section of the gravity meter. The ultra sensitive Zero Length Spring balances the Mass on the balance Beam. The galvanometer 'beam' measures the Long Lever location with respect to zero.

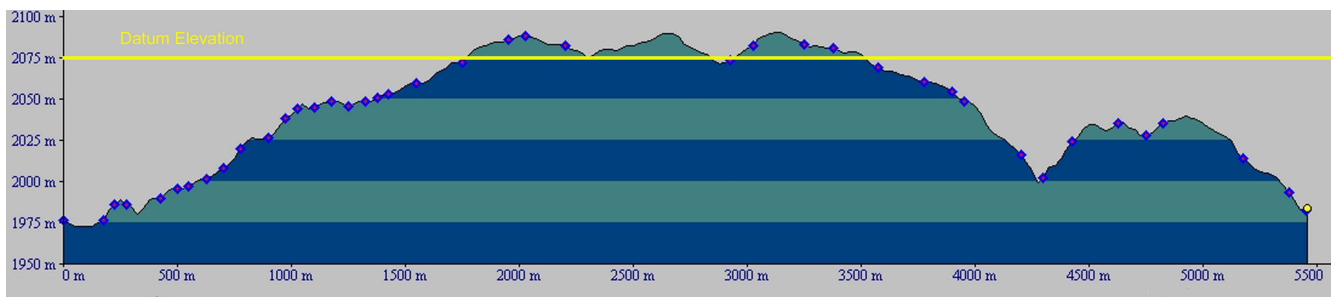


Figure 11 Elevation profile along Silver Spur Rd starting at the mail boxes on the County Rd 330 and ending at the south entrance. Yellow line shows gravity datum elevation at 2076m. Vertical exaggeration is a factor of 12.

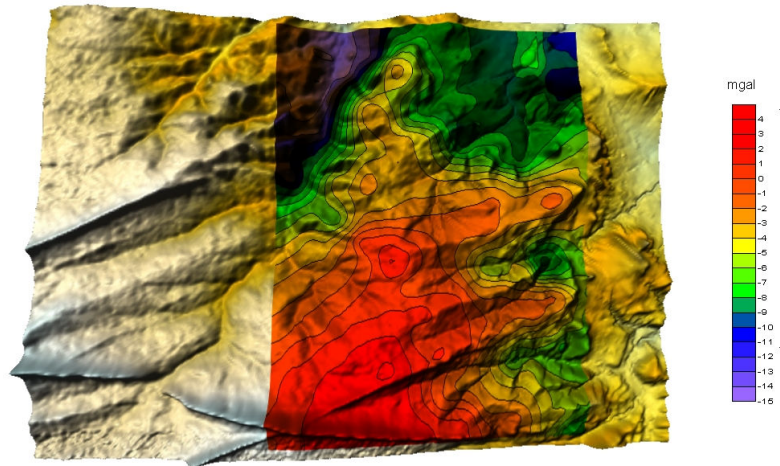


Figure 12 Free air anomaly map shown with regional topography. Red gravity anomaly contours trend along surface ridges.

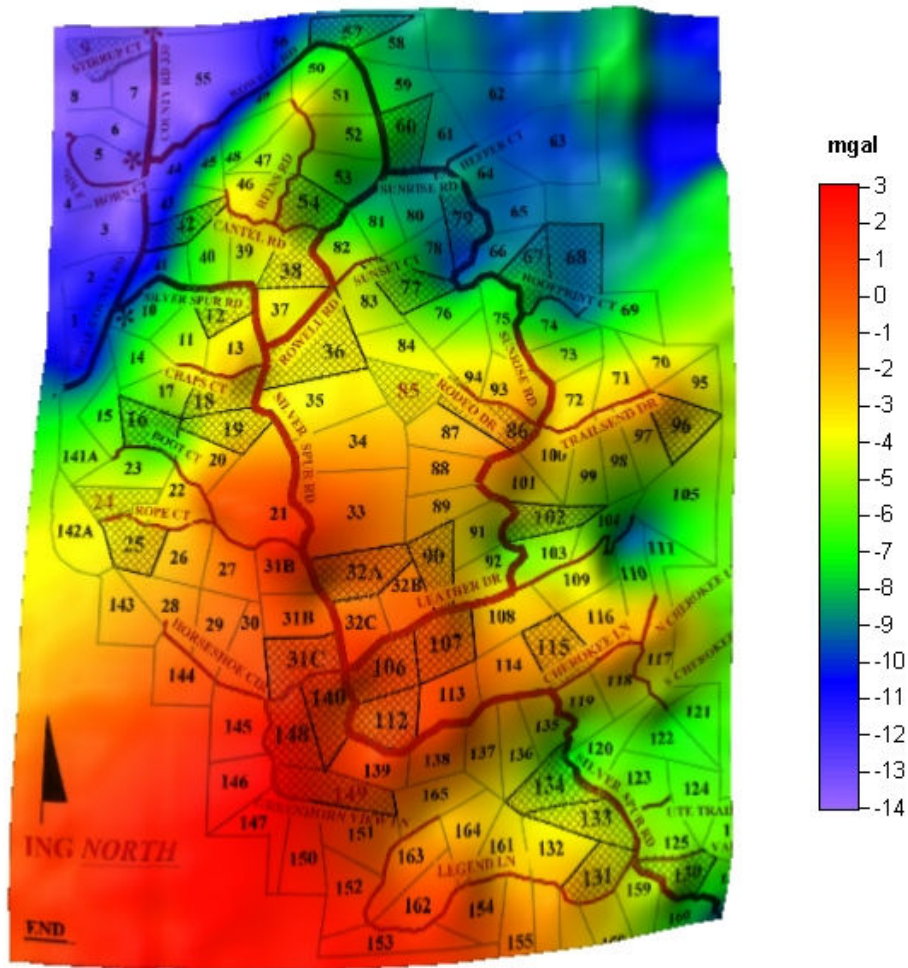


Figure 13 Free air anomaly map shown with property map.

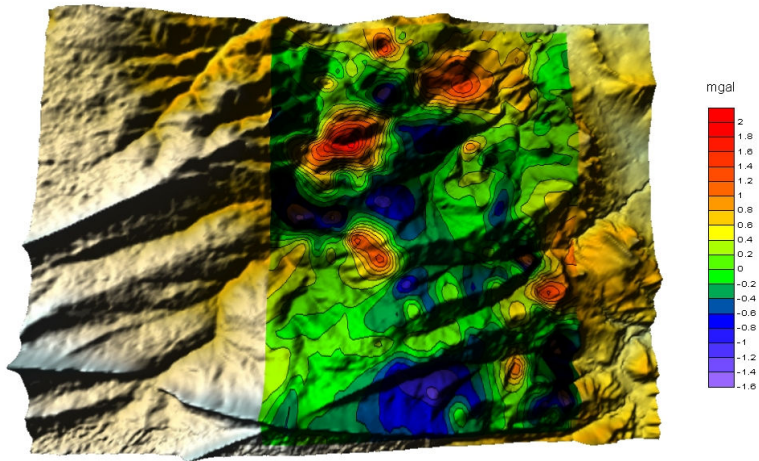


Figure 14 Bouguer anomaly map shown with regional topography.

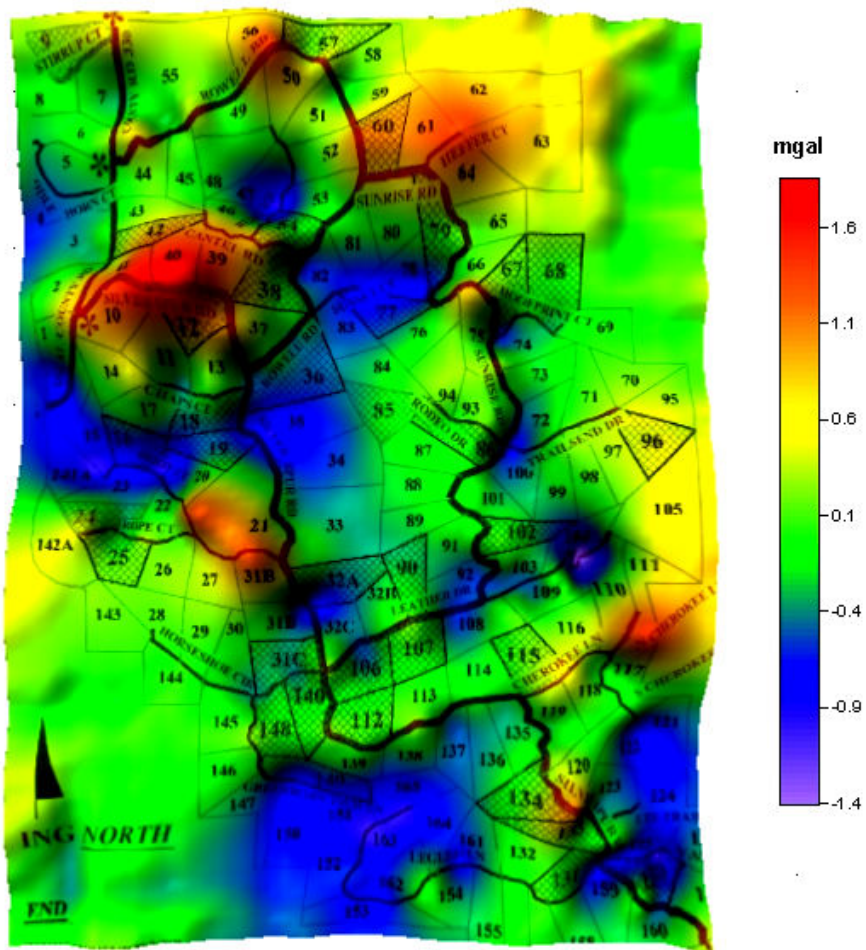


Figure 15 Bouguer anomaly map with property map.

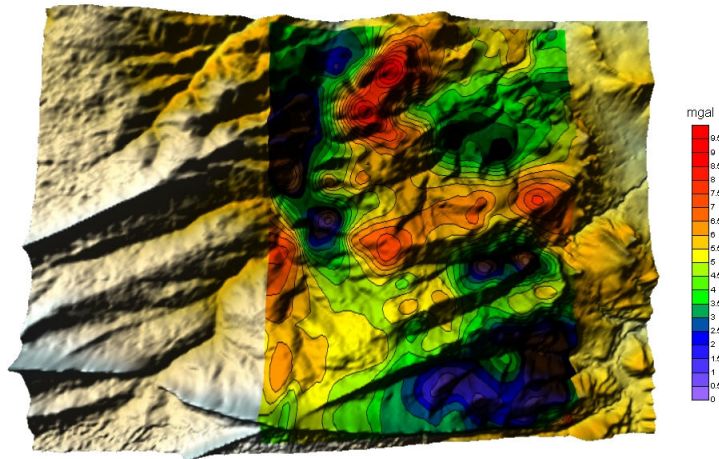


Figure 16 Complete Bouguer anomaly map shown with regional topography.

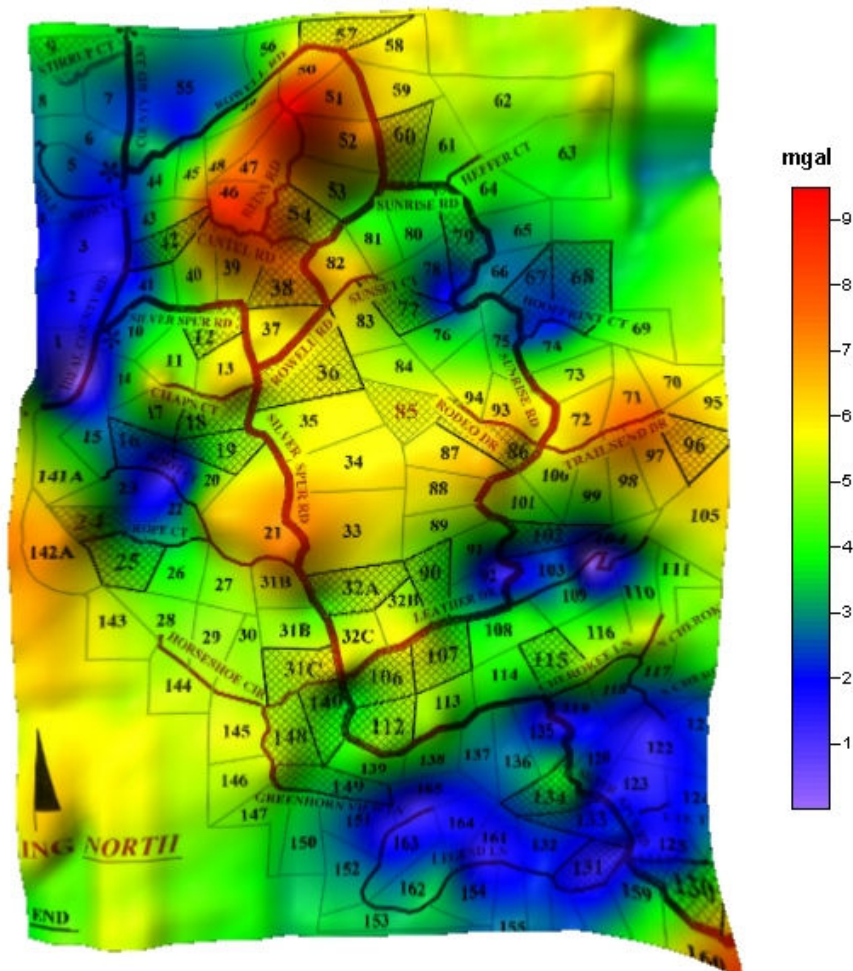


Figure 17 Complete Bouguer anomaly map with property map.

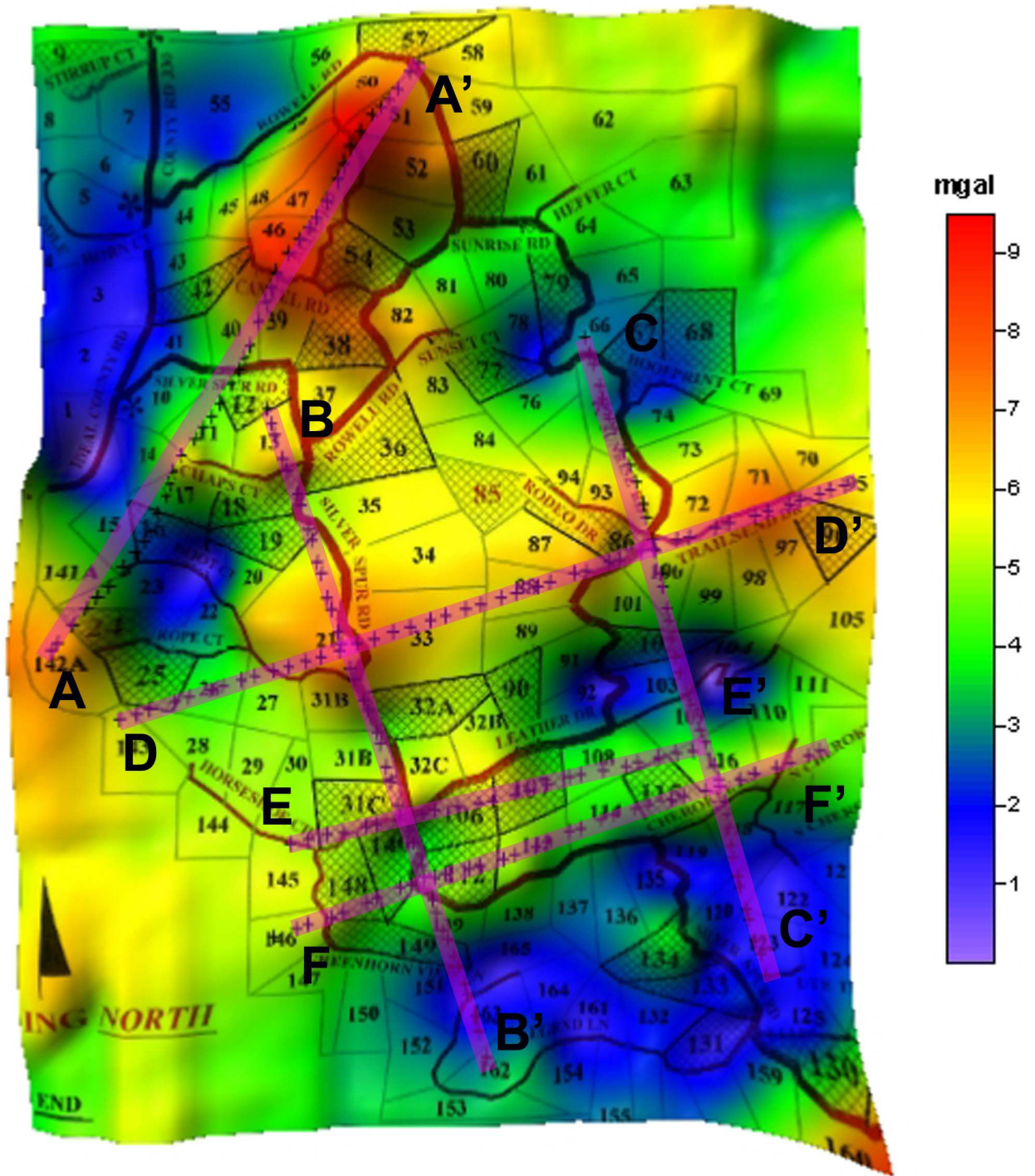


Figure 18 Complete Bouguer anomaly map with gravity modeling profiles.

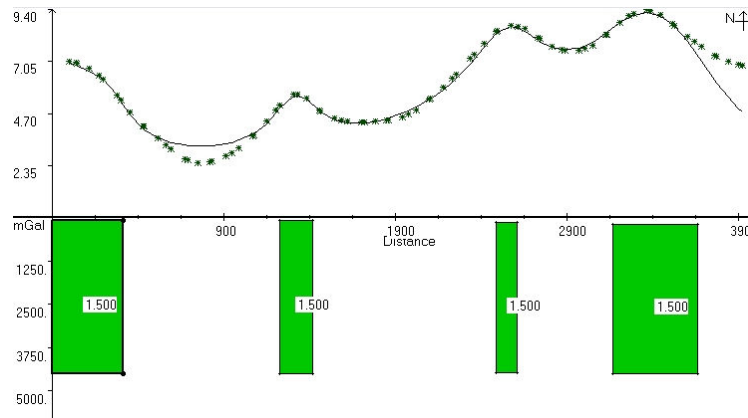


Figure 19 Profile AA', Rope Ct to Reins Rd.

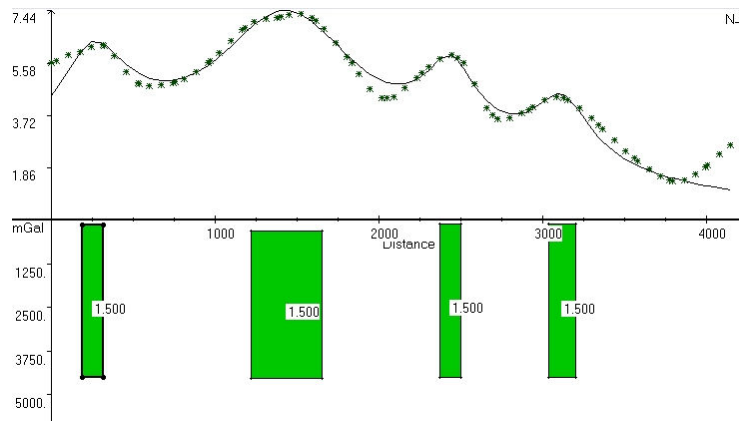


Figure 20 Profile BB', north end of Silver Spurs Rd.

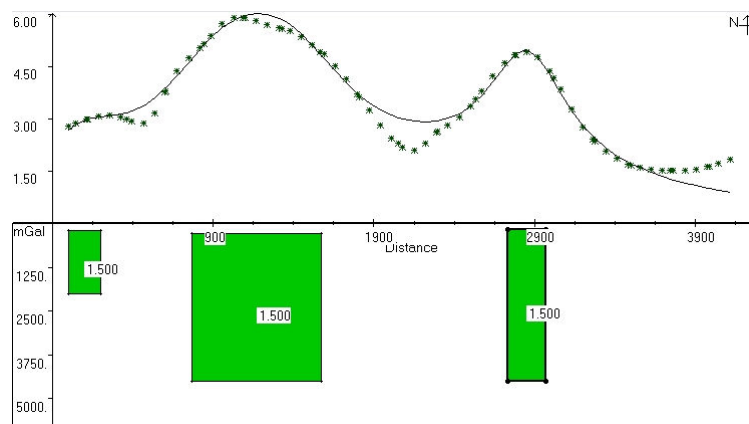


Figure 21 Profile CC', Sunrise Rd to south Silver Spurs Rd.

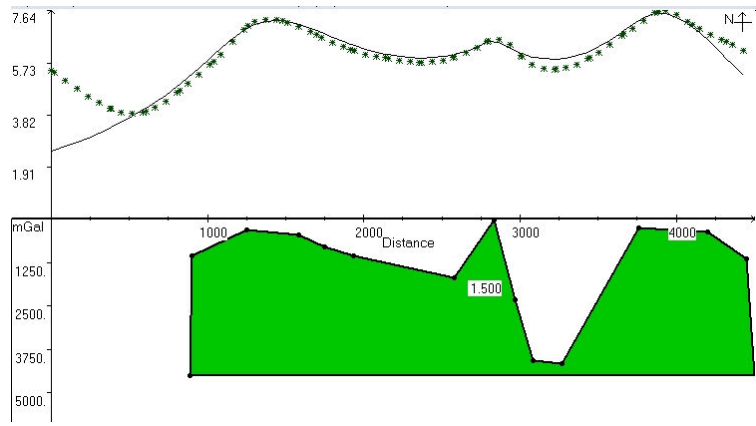


Figure 22 Profile DD', Rope Ct to Trails End Dr.

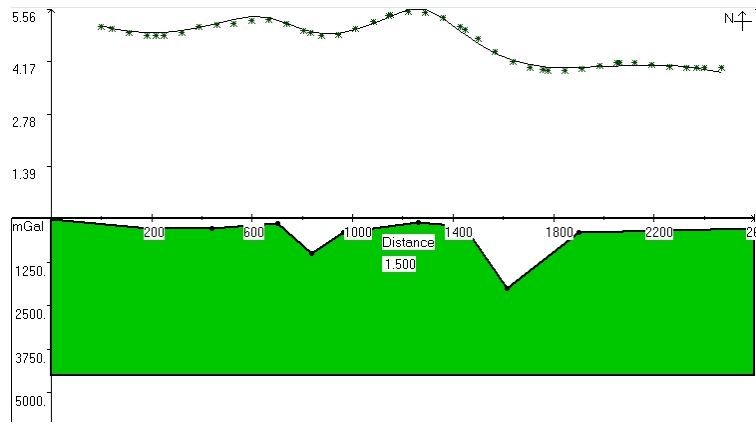


Figure 23 Profile EE', Horseshoe Ct to Leather Dr.

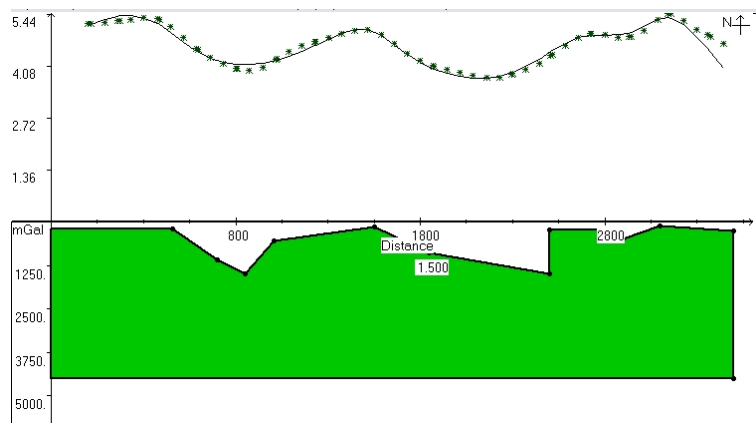


Figure 24 Profile FF', Green Horn View Ln to Cherokee Ln.

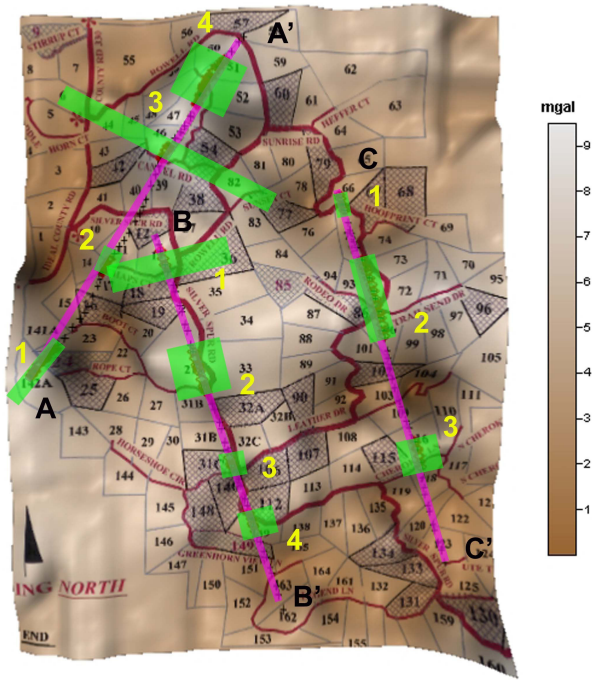


Figure 25 Lateral position of constant density gravity blocks marked in green.

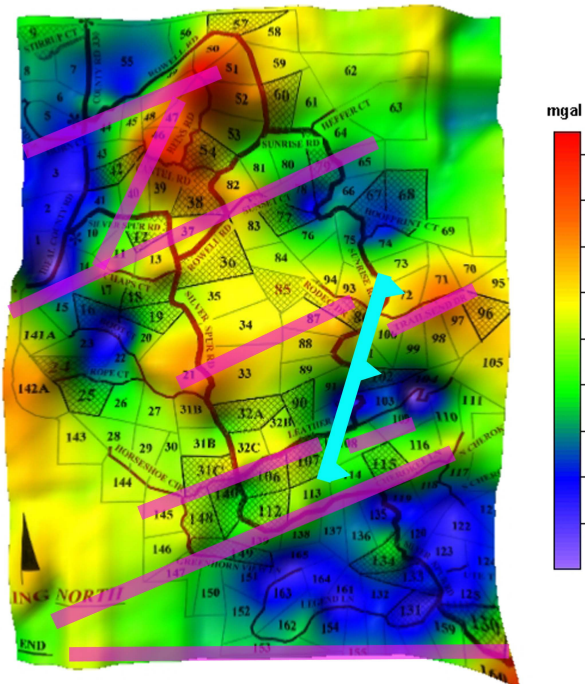


Figure 26 Final interpretations of dike locations. NNE trending fault in cyan is shown extending from Sunrise Rd to Leather Dr.

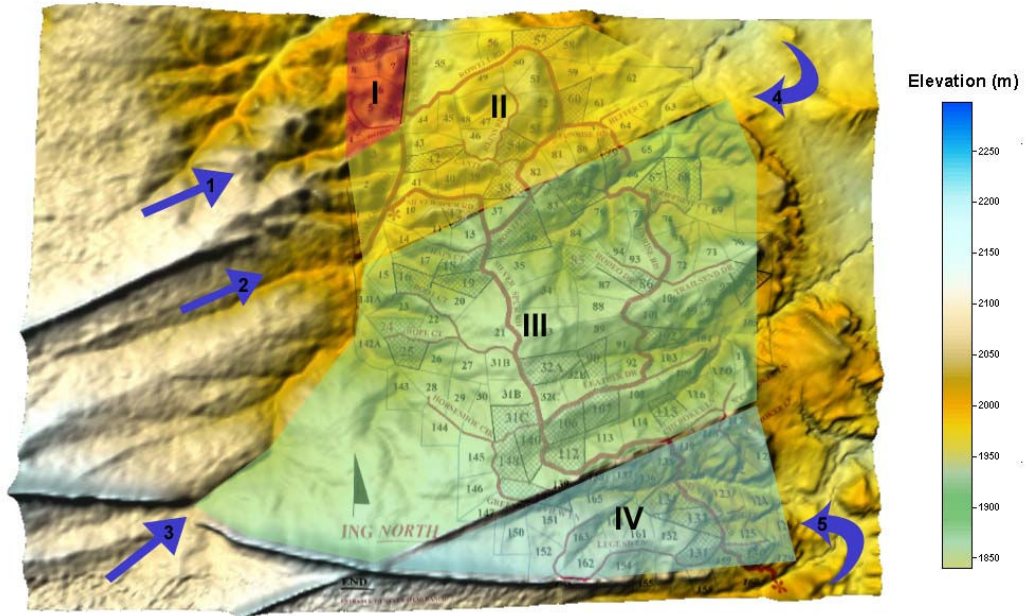


Figure 27 Water regions with recharge areas marked with blue arrows.

Appendix A

Gravity correction formulas

Drift correction:

$$g_{dc} = g_{obs} - [(g_{base2} - g_{base1}) / (t_{base2} - t_{base1})] \times (t_{obs} - t_{base1})$$

g_{obs} = observed gravity

g_{base} = gravity at base station

t_{obs} = time of gravity observation

t_{base} = time of observation at base station

Latitude correction:

$$g_{IGF} = 9.78032[(1 + 0.00193185138\sin^2 \lambda) / (1 - .006694379\sin^2 \lambda)^{1/2}]$$

λ = geographic latitude in radians

Free air correction:

$$g_{FA} = 0.3086 * (\text{surface elevation} - \text{datum elevation}) \quad \text{elevation in meters}$$

Bouguer correction:

$$g_B = g_{FA} - 0.04193 * \text{density} * (\text{surface elevation} - \text{datum elevation})$$

for an average density of 2.67 g/cc

$$g_B = g_{FA} - 0.112 * (\text{surface elevation} - \text{datum elevation})$$

$$g_B = 0.1966 * (\text{surface elevation} - \text{datum elevation}) \quad \text{elevation in meters}$$

Complete Bouguer correction:

$$g_{CB} = g_{dc} - g_{IGF} + g_B + \text{terrain correction}$$

Appendix B

Table 2 Gravity measurements and corrections.

Gravity units are in mgal. UTM XY locations and elevations are in meters.

| <i>stn</i> | <i>x</i> | <i>y</i> | <i>elev</i> | <i>field g</i> | <i>rel g</i> | <i>latitude</i> | <i>free air</i> | <i>bouguer</i> | <i>complete</i> |
|------------|----------|----------|-------------|----------------|--------------|-----------------|-----------------|----------------|-----------------|
| B1 | 522518 | 4152400 | 2076 | 913.10 | 106.15 | 106.15 | 106.15 | 106.15 | 111.82 |
| 1 | 522501 | 4152445 | 2075 | 917.76 | 106.71 | 106.68 | 106.37 | 106.48 | 111.56 |
| 2 | 522603 | 4152467 | 2069 | 924.49 | 107.54 | 107.48 | 105.32 | 106.11 | 110.48 |
| 3 | 522703 | 4152480 | 2065 | 927.15 | 107.86 | 107.80 | 104.41 | 105.64 | 109.81 |
| 4 | 522806 | 4152490 | 2060 | 933.81 | 108.65 | 108.59 | 103.65 | 105.44 | 109.64 |
| 5 | 522905 | 4152503 | 2060 | 935.13 | 108.86 | 108.78 | 103.84 | 105.63 | 109.57 |
| 6 | 522998 | 4152533 | 2057 | 941.69 | 109.65 | 109.54 | 103.68 | 105.81 | 109.41 |
| 7 | 523092 | 4152572 | 2053 | 952.82 | 110.98 | 110.84 | 103.74 | 106.32 | 109.84 |
| 8 | 523186 | 4152602 | 2051 | 960.67 | 111.83 | 111.67 | 103.96 | 106.76 | 110.05 |
| 9 | 523280 | 4152639 | 2049 | 962.05 | 111.97 | 111.78 | 103.45 | 106.47 | 109.12 |
| 10 | 523373 | 4152678 | 2042 | 969.12 | 112.77 | 112.55 | 102.06 | 105.86 | 108.30 |
| 11 | 523457 | 4152730 | 2039 | 976.83 | 113.64 | 113.38 | 101.96 | 106.11 | 109.01 |
| 12 | 523546 | 4152775 | 2040 | 987.61 | 114.87 | 114.58 | 103.47 | 107.50 | 109.80 |
| 13 | 523639 | 4152816 | 2036 | 985.36 | 114.59 | 114.27 | 101.92 | 106.40 | 108.03 |
| 14 | 523720 | 4152875 | 2028 | 997.12 | 115.94 | 115.57 | 100.76 | 106.13 | 106.58 |
| 15 | 523786 | 4152916 | 2015 | 1005.54 | 116.90 | 116.49 | 97.67 | 104.50 | 104.78 |
| 16 | 523752 | 4152827 | 2013 | 1016.13 | 118.11 | 117.78 | 98.34 | 105.39 | 105.56 |
| 17 | 523832 | 4152855 | 2005 | 1038.55 | 120.69 | 120.34 | 98.43 | 106.38 | 106.74 |
| 18 | 523916 | 4152903 | 1999 | 1050.88 | 122.11 | 121.71 | 97.95 | 106.57 | 107.23 |
| 19 | 523976 | 4152989 | 1993 | 1062.21 | 123.40 | 122.94 | 97.33 | 106.62 | 107.25 |
| 20 | 524000 | 4153076 | 1992 | 1073.76 | 124.73 | 124.20 | 98.28 | 107.68 | 110.99 |
| 21 | 523056 | 4152638 | 2049 | 963.36 | 111.84 | 111.65 | 103.32 | 106.34 | 108.80 |
| 22 | 523078 | 4152738 | 2039 | 975.30 | 113.22 | 112.95 | 101.53 | 105.68 | 107.28 |
| 23 | 523150 | 4152801 | 2029 | 993.36 | 115.31 | 115.00 | 100.49 | 105.75 | 107.38 |
| 24 | 523097 | 4152873 | 2028 | 1005.85 | 116.75 | 116.38 | 101.57 | 106.94 | 107.70 |
| 25 | 523017 | 4152921 | 2017 | 1017.21 | 118.07 | 117.66 | 99.45 | 106.05 | 107.71 |
| 26 | 522990 | 4153015 | 2026 | 1008.03 | 116.98 | 116.49 | 101.06 | 106.66 | 109.52 |
| 27 | 523049 | 4153095 | 2034 | 1000.71 | 116.12 | 115.57 | 102.61 | 107.31 | 110.52 |
| 28 | 523089 | 4153173 | 2039 | 991.64 | 115.05 | 114.45 | 103.03 | 107.17 | 111.09 |
| 29 | 523007 | 4153234 | 2045 | 977.50 | 113.40 | 112.75 | 103.18 | 106.65 | 111.38 |
| 30 | 522920 | 4153281 | 2052 | 973.68 | 112.60 | 111.91 | 104.50 | 107.19 | 112.46 |
| 31 | 522847 | 4153346 | 2056 | 967.56 | 111.92 | 111.18 | 105.00 | 107.24 | 112.83 |
| 32 | 522829 | 4153424 | 2061 | 956.99 | 110.72 | 109.92 | 105.29 | 106.97 | 113.25 |
| 33 | 522884 | 4153514 | 2066 | 952.55 | 110.23 | 109.36 | 106.27 | 107.39 | 114.31 |
| 34 | 522970 | 4153557 | 2068 | 950.34 | 110.00 | 109.09 | 106.62 | 107.51 | 114.19 |
| 35 | 523062 | 4153598 | 2065 | 950.66 | 110.06 | 109.12 | 105.72 | 106.96 | 113.04 |
| 36 | 523151 | 4153650 | 2062 | 957.13 | 110.83 | 109.85 | 105.53 | 107.10 | 112.88 |
| 37 | 523230 | 4153772 | 2057 | 966.48 | 111.65 | 110.57 | 104.71 | 106.84 | 113.51 |
| 38 | 523146 | 4153831 | 2061 | 963.71 | 111.54 | 110.41 | 105.79 | 107.46 | 114.25 |
| 39 | 523063 | 4153894 | 2061 | 971.36 | 112.40 | 111.22 | 106.59 | 108.27 | 114.55 |
| 40 | 522975 | 4153931 | 2059 | 974.51 | 112.73 | 111.53 | 106.28 | 108.18 | 114.63 |
| 41 | 522871 | 4153945 | 2057 | 975.50 | 112.80 | 111.59 | 105.72 | 107.85 | 114.16 |
| 42 | 522782 | 4153982 | 2055 | 978.42 | 113.12 | 111.87 | 105.39 | 107.74 | 113.79 |

| <i>stn</i> | <i>x</i> | <i>y</i> | <i>elev</i> | <i>field g</i> | <i>rel g</i> | <i>latitude</i> | <i>free air</i> | <i>bouguer</i> | <i>complete</i> |
|------------|----------|----------|-------------|----------------|--------------|-----------------|-----------------|----------------|-----------------|
| 43 | 522688 | 4154074 | 2051 | 990.52 | 114.49 | 113.17 | 105.46 | 108.26 | 114.10 |
| 44 | 523330 | 4153737 | 2055 | 973.72 | 112.51 | 111.45 | 104.97 | 107.32 | 113.16 |
| 45 | 523429 | 4153732 | 2055 | 976.64 | 112.84 | 111.79 | 105.31 | 107.66 | 113.56 |
| 46 | 523524 | 4153766 | 2055 | 980.32 | 113.26 | 112.19 | 105.71 | 108.06 | 113.56 |
| 47 | 523605 | 4153821 | 2057 | 980.95 | 113.33 | 112.22 | 106.35 | 108.48 | 114.47 |
| 48 | 523693 | 4153870 | 2054 | 983.60 | 113.64 | 112.48 | 105.69 | 108.16 | 114.52 |
| 49 | 523788 | 4153892 | 2057 | 982.16 | 113.47 | 112.30 | 106.43 | 108.56 | 115.17 |
| 50 | 523883 | 4153920 | 2059 | 978.85 | 113.08 | 111.89 | 106.64 | 108.54 | 115.70 |
| 51 | 524007 | 4153978 | 2063 | 975.26 | 112.66 | 111.42 | 107.41 | 108.86 | 115.03 |
| 52 | 523285 | 4153856 | 2056 | 971.09 | 112.12 | 110.97 | 104.80 | 107.04 | 113.03 |
| 53 | 523325 | 4153950 | 2056 | 976.93 | 112.73 | 111.51 | 105.34 | 107.58 | 113.70 |
| 54 | 523325 | 4154050 | 2052 | 984.91 | 113.61 | 112.32 | 104.91 | 107.60 | 113.63 |
| 55 | 523254 | 4154124 | 2050 | 992.28 | 114.42 | 113.07 | 105.04 | 107.95 | 113.71 |
| 56 | 523190 | 4154207 | 2046 | 1001.95 | 115.49 | 114.06 | 104.81 | 108.16 | 112.89 |
| 57 | 523156 | 4154299 | 2038 | 1020.28 | 117.55 | 116.06 | 104.33 | 108.59 | 112.97 |
| 58 | 523119 | 4154391 | 2030 | 1039.73 | 119.75 | 118.19 | 103.99 | 109.14 | 112.56 |
| 59 | 523104 | 4154499 | 2019 | 1050.13 | 120.90 | 119.25 | 101.66 | 108.04 | 111.08 |
| 60 | 523149 | 4154578 | 2014 | 1057.98 | 121.76 | 120.04 | 100.91 | 107.85 | 110.29 |
| 61 | 523235 | 4154638 | 2007 | 1075.24 | 123.72 | 121.96 | 100.66 | 108.39 | 110.54 |
| 62 | 523293 | 4154714 | 2000 | 1090.13 | 125.40 | 123.58 | 100.13 | 108.64 | 110.42 |
| 63 | 523399 | 4154718 | 1999 | 1095.85 | 126.01 | 124.19 | 100.43 | 109.05 | 110.75 |
| 64 | 523485 | 4154674 | 1996 | 1095.44 | 125.91 | 124.12 | 99.43 | 108.39 | 109.63 |
| 65 | 523562 | 4154587 | 1995 | 1100.50 | 126.46 | 124.74 | 99.74 | 108.81 | 111.61 |
| 66 | 523123 | 4154685 | 2013 | 1067.29 | 122.50 | 120.71 | 101.26 | 108.32 | 111.48 |
| 67 | 523106 | 4154780 | 2012 | 1076.97 | 123.57 | 121.70 | 101.95 | 109.12 | 111.46 |
| 68 | 523021 | 4154837 | 2003 | 1097.94 | 125.95 | 124.03 | 101.50 | 109.67 | 111.41 |
| 69 | 522938 | 4154894 | 1996 | 1109.33 | 127.27 | 125.31 | 100.62 | 109.57 | 111.57 |
| 70 | 522847 | 4154873 | 1999 | 1110.72 | 127.43 | 125.48 | 101.72 | 110.34 | 112.18 |
| 71 | 522753 | 4154827 | 1998 | 1105.29 | 126.80 | 124.89 | 100.82 | 109.55 | 111.03 |
| 72 | 522666 | 4154838 | 1994 | 1105.29 | 126.80 | 124.88 | 99.57 | 108.75 | 110.16 |
| 73 | 522651 | 4154928 | 1992 | 1104.80 | 126.74 | 124.75 | 98.82 | 108.23 | 109.81 |
| 74 | 522724 | 4154999 | 1993 | 1107.83 | 127.34 | 125.29 | 99.68 | 108.97 | 110.63 |
| 75 | 522787 | 4155075 | 1990 | 1108.04 | 127.36 | 125.25 | 98.71 | 108.34 | 110.52 |
| 76 | 522819 | 4155167 | 1997 | 1110.58 | 127.65 | 125.47 | 101.09 | 109.93 | 112.37 |
| 77 | 522897 | 4155225 | 1996 | 1109.29 | 127.49 | 125.27 | 100.58 | 109.53 | 111.51 |
| 78 | 522891 | 4155317 | 1993 | 1115.88 | 128.25 | 125.95 | 100.34 | 109.63 | 111.29 |
| 80 | 522764 | 4155469 | 1991 | 1123.85 | 129.17 | 126.75 | 100.52 | 110.04 | 112.49 |
| 81 | 522721 | 4155563 | 1995 | 1123.65 | 129.14 | 126.65 | 101.65 | 110.72 | 112.68 |
| 79 | 522845 | 4155402 | 1992 | 1121.27 | 128.85 | 126.49 | 100.57 | 109.97 | 112.32 |
| 82 | 522659 | 4155638 | 1993 | 1128.18 | 129.65 | 127.10 | 101.48 | 110.78 | 112.88 |
| 83 | 522575 | 4155681 | 1990 | 1136.13 | 130.56 | 127.98 | 101.44 | 111.07 | 112.57 |
| 84 | 522616 | 4155758 | 1984 | 1147.90 | 131.92 | 129.28 | 100.89 | 111.19 | 112.59 |
| 85 | 522707 | 4155807 | 1981 | 1155.94 | 132.85 | 130.17 | 100.85 | 111.49 | 112.78 |
| 86 | 522803 | 4155866 | 1979 | 1161.76 | 133.52 | 130.79 | 100.86 | 111.72 | 113.64 |
| 87 | 522460 | 4155691 | 1988 | 1136.46 | 130.57 | 127.98 | 100.82 | 110.67 | 112.78 |
| 88 | 522360 | 4155686 | 1990 | 1132.73 | 130.13 | 127.54 | 101.00 | 110.63 | 112.82 |
| 89 | 522262 | 4155670 | 1991 | 1130.68 | 129.88 | 127.31 | 101.08 | 110.59 | 113.58 |

| <i>stn</i> | <i>x</i> | <i>y</i> | <i>elev</i> | <i>field g</i> | <i>rel g</i> | <i>latitude</i> | <i>free air</i> | <i>bouguer</i> | <i>complete</i> |
|------------|----------|----------|-------------|----------------|--------------|-----------------|-----------------|----------------|-----------------|
| 90 | 522131 | 4155670 | 1999 | 1117.25 | 128.31 | 125.74 | 101.97 | 110.59 | 113.81 |
| 91 | 522142 | 4155772 | 2000 | 1118.02 | 128.37 | 125.72 | 102.26 | 110.77 | 114.65 |
| 92 | 522123 | 4155874 | 2005 | 1115.08 | 128.02 | 125.29 | 103.38 | 111.32 | 115.85 |
| 93 | 522093 | 4155970 | 2010 | 1105.46 | 126.90 | 124.09 | 103.72 | 111.11 | 115.77 |
| 94 | 522066 | 4156055 | 2010 | 1100.80 | 126.35 | 123.47 | 103.10 | 110.49 | 114.96 |
| 95 | 522042 | 4156151 | 2007 | 1109.04 | 127.30 | 124.35 | 103.05 | 110.78 | 115.34 |
| 96 | 522016 | 4156250 | 2010 | 1100.68 | 126.32 | 123.29 | 102.92 | 110.31 | 115.32 |
| 97 | 521989 | 4156345 | 2010 | 1098.83 | 126.10 | 122.99 | 102.62 | 110.01 | 115.12 |
| 98 | 521927 | 4156433 | 2010 | 1100.97 | 126.34 | 123.17 | 102.80 | 110.19 | 115.60 |
| 99 | 521860 | 4156507 | 2012 | 1108.65 | 127.23 | 123.99 | 104.24 | 111.41 | 115.77 |
| 100 | 521775 | 4156561 | 2004 | 1114.43 | 127.89 | 124.62 | 102.40 | 110.46 | 114.26 |
| 101 | 521681 | 4156590 | 1999 | 1120.22 | 128.56 | 125.26 | 101.50 | 110.12 | 114.24 |
| 102 | 521588 | 4156573 | 1999 | 1129.98 | 129.69 | 126.40 | 102.64 | 111.26 | 114.68 |
| 103 | 521512 | 4156510 | 1993 | 1144.28 | 131.34 | 128.10 | 102.49 | 111.78 | 114.22 |
| 104 | 521420 | 4156456 | 1987 | 1151.66 | 132.19 | 129.00 | 101.53 | 111.49 | 113.72 |
| 105 | 521326 | 4156411 | 1981 | 1157.23 | 132.84 | 129.68 | 100.37 | 111.00 | 112.84 |
| 106 | 521235 | 4156376 | 1976 | 1158.92 | 133.04 | 129.91 | 99.05 | 110.25 | 111.45 |
| 107 | 521140 | 4156344 | 1972 | 1160.67 | 133.25 | 130.14 | 98.05 | 109.69 | 110.79 |
| 108 | 521045 | 4156309 | 1971 | 1166.16 | 133.89 | 130.81 | 98.41 | 110.16 | 110.98 |
| 109 | 520969 | 4156244 | 1971 | 1162.23 | 133.44 | 130.41 | 98.01 | 109.76 | 110.44 |
| 110 | 520884 | 4156187 | 1967 | 1178.76 | 135.37 | 132.38 | 98.75 | 110.95 | 111.14 |
| 111 | 520794 | 4156144 | 1959 | 1180.77 | 135.60 | 132.65 | 96.55 | 109.64 | 109.79 |
| 112 | 520692 | 4156136 | 1955 | 1182.74 | 135.84 | 132.89 | 95.55 | 109.10 | 109.23 |
| 113 | 520610 | 4156075 | 1957 | 1183.97 | 135.98 | 133.09 | 96.36 | 109.68 | 109.83 |
| 114 | 520535 | 4156010 | 1957 | 1189.74 | 136.66 | 133.81 | 97.09 | 110.41 | 110.85 |
| 115 | 520443 | 4155977 | 1950 | 1202.01 | 138.09 | 135.27 | 96.38 | 110.49 | 110.91 |
| 116 | 520360 | 4155923 | 1951 | 1191.48 | 136.87 | 134.09 | 95.51 | 109.51 | 109.62 |
| 117 | 520279 | 4155943 | 1960 | 1179.03 | 135.42 | 132.63 | 96.83 | 109.82 | 112.96 |
| 118 | 522037 | 4155555 | 1999 | 1109.63 | 127.40 | 124.92 | 101.16 | 109.78 | 112.64 |
| 119 | 521944 | 4155492 | 2000 | 1103.66 | 126.72 | 124.29 | 100.83 | 109.34 | 112.43 |
| 120 | 521862 | 4155429 | 2003 | 1099.33 | 126.23 | 123.84 | 101.31 | 109.49 | 112.77 |
| 121 | 521805 | 4155346 | 2009 | 1089.06 | 125.04 | 122.72 | 102.04 | 109.55 | 113.58 |
| 122 | 521739 | 4155268 | 2014 | 1073.88 | 123.29 | 121.03 | 101.90 | 108.84 | 113.65 |
| 123 | 521664 | 4155223 | 2022 | 1060.48 | 121.74 | 119.52 | 102.85 | 108.90 | 113.94 |
| 124 | 521541 | 4155238 | 2024 | 1065.32 | 122.31 | 120.08 | 104.03 | 109.85 | 115.68 |
| 125 | 521438 | 4155193 | 2032 | 1053.14 | 120.91 | 118.71 | 105.13 | 110.05 | 116.46 |
| 126 | 521351 | 4155221 | 2037 | 1042.76 | 119.71 | 117.49 | 105.46 | 109.82 | 116.66 |
| 127 | 521348 | 4155313 | 2040 | 1038.06 | 119.18 | 116.88 | 105.77 | 109.80 | 116.76 |
| 128 | 521364 | 4155409 | 2040 | 1030.20 | 118.27 | 115.90 | 104.79 | 108.82 | 115.81 |
| 129 | 521408 | 4155513 | 2039 | 1030.62 | 118.33 | 115.88 | 104.46 | 108.60 | 115.60 |
| 130 | 521462 | 4155604 | 2038 | 1031.67 | 118.46 | 115.94 | 104.21 | 108.46 | 115.48 |
| 131 | 521509 | 4155694 | 2037 | 1035.18 | 118.88 | 116.28 | 104.25 | 108.61 | 116.05 |
| 132 | 521574 | 4155770 | 2040 | 1035.60 | 118.93 | 116.28 | 105.17 | 109.20 | 116.99 |
| 133 | 521600 | 4155870 | 2042 | 1032.89 | 118.63 | 115.90 | 105.40 | 109.21 | 117.46 |
| 134 | 521569 | 4155966 | 2045 | 1036.47 | 119.06 | 116.25 | 106.68 | 110.15 | 118.42 |
| 135 | 521499 | 4156044 | 2044 | 1037.74 | 119.22 | 116.35 | 106.48 | 110.06 | 117.75 |
| 136 | 521443 | 4156129 | 2041 | 1045.04 | 120.07 | 117.13 | 106.33 | 110.25 | 117.20 |

| <i>stn</i> | <i>x</i> | <i>y</i> | <i>elev</i> | <i>field g</i> | <i>rel g</i> | <i>latitude</i> | <i>free air</i> | <i>bouguer</i> | <i>complete</i> |
|------------|----------|----------|-------------|----------------|--------------|-----------------|-----------------|----------------|-----------------|
| 137 | 521231 | 4155233 | 2042 | 1035.18 | 118.93 | 116.70 | 106.20 | 110.01 | 116.56 |
| 138 | 521144 | 4155285 | 2041 | 1037.79 | 119.23 | 116.96 | 106.16 | 110.08 | 117.15 |
| 139 | 521043 | 4155329 | 2042 | 1033.88 | 118.78 | 116.47 | 105.98 | 109.79 | 116.56 |
| 140 | 520993 | 4155429 | 2038 | 1043.28 | 119.88 | 117.49 | 105.76 | 110.02 | 116.47 |
| 141 | 520961 | 4155512 | 2034 | 1043.67 | 119.92 | 117.47 | 104.51 | 109.21 | 115.13 |
| 142 | 521618 | 4155101 | 2034 | 1031.88 | 118.56 | 116.43 | 103.47 | 108.17 | 115.02 |
| 143 | 521599 | 4155011 | 2044 | 1017.24 | 116.86 | 114.80 | 104.92 | 108.51 | 115.77 |
| 144 | 521666 | 4154931 | 2049 | 1008.66 | 115.86 | 113.87 | 105.53 | 108.56 | 115.62 |
| 145 | 521726 | 4154852 | 2048 | 1009.29 | 115.94 | 114.00 | 105.36 | 108.50 | 115.04 |
| 146 | 521743 | 4154795 | 2044 | 1010.90 | 116.12 | 114.24 | 104.36 | 107.95 | 114.02 |
| 147 | 521831 | 4154867 | 2042 | 1018.30 | 116.99 | 115.04 | 104.55 | 108.36 | 114.88 |
| 148 | 521916 | 4154934 | 2042 | 1018.49 | 117.01 | 115.01 | 104.52 | 108.33 | 114.93 |
| 149 | 522009 | 4154984 | 2042 | 1017.60 | 116.91 | 114.87 | 104.38 | 108.19 | 115.14 |
| 150 | 521678 | 4154719 | 2049 | 1008.91 | 115.90 | 114.07 | 105.74 | 108.76 | 115.29 |
| 151 | 521609 | 4154646 | 2046 | 1009.23 | 115.94 | 114.17 | 104.91 | 108.27 | 114.59 |
| 152 | 521536 | 4154576 | 2042 | 1009.95 | 116.03 | 114.31 | 103.82 | 107.62 | 113.47 |
| 153 | 521468 | 4154500 | 2042 | 1017.22 | 116.87 | 115.22 | 104.73 | 108.53 | 114.47 |
| 154 | 521392 | 4154433 | 2044 | 1010.84 | 116.13 | 114.53 | 104.65 | 108.24 | 113.91 |
| 155 | 521249 | 4154370 | 2046 | 1002.21 | 115.13 | 113.58 | 104.32 | 107.68 | 113.23 |
| 156 | 521209 | 4154473 | 2043 | 1021.91 | 117.38 | 115.74 | 105.56 | 109.25 | 114.48 |
| 157 | 521190 | 4154573 | 2035 | 1038.27 | 119.27 | 117.55 | 104.90 | 109.49 | 114.25 |
| 158 | 521182 | 4154678 | 2029 | 1044.54 | 119.98 | 118.19 | 103.68 | 108.94 | 113.36 |
| 159 | 521170 | 4154791 | 2024 | 1062.05 | 122.01 | 120.12 | 104.07 | 109.89 | 113.74 |
| 160 | 521077 | 4154830 | 2018 | 1071.43 | 123.08 | 121.17 | 103.27 | 109.76 | 113.09 |
| 161 | 520977 | 4154831 | 2013 | 1090.12 | 125.24 | 123.33 | 103.88 | 110.94 | 113.75 |
| 162 | 520874 | 4154822 | 2007 | 1095.90 | 125.90 | 123.99 | 102.70 | 110.42 | 112.44 |
| 163 | 520777 | 4154827 | 2000 | 1107.31 | 127.22 | 125.30 | 101.85 | 110.36 | 111.91 |
| 164 | 520663 | 4154829 | 1995 | 1116.02 | 128.21 | 126.30 | 101.30 | 110.37 | 111.53 |
| 165 | 520572 | 4154869 | 1990 | 1124.10 | 129.14 | 127.20 | 100.66 | 110.28 | 111.01 |
| 166 | 520482 | 4154913 | 1984 | 1134.21 | 130.30 | 128.32 | 99.93 | 110.23 | 110.38 |
| 167 | 520367 | 4154950 | 1973 | 1143.90 | 131.41 | 129.40 | 97.61 | 109.14 | 109.37 |
| 168 | 520272 | 4154891 | 1976 | 1146.40 | 131.68 | 129.72 | 98.86 | 110.05 | 110.18 |
| 169 | 520183 | 4154835 | 1972 | 1145.06 | 131.52 | 129.59 | 97.50 | 109.14 | 109.30 |
| 170 | 520027 | 4154750 | 1976 | 1138.61 | 130.75 | 128.89 | 98.03 | 109.23 | 109.37 |
| 171 | 520312 | 4156849 | 1950 | 1208.63 | 138.85 | 135.34 | 96.46 | 110.56 | 110.76 |
| 172 | 520314 | 4156744 | 1946 | 1211.01 | 139.12 | 135.70 | 95.58 | 110.13 | 110.27 |
| 173 | 520314 | 4156638 | 1949 | 1209.75 | 138.97 | 135.63 | 96.44 | 110.65 | 110.78 |
| 174 | 520312 | 4156538 | 1951 | 1199.17 | 137.74 | 134.47 | 95.90 | 109.89 | 110.03 |
| 175 | 520309 | 4156429 | 1952 | 1192.18 | 136.92 | 133.74 | 95.47 | 109.36 | 109.48 |
| 176 | 520306 | 4156333 | 1955 | 1185.16 | 136.10 | 133.00 | 95.66 | 109.20 | 109.38 |
| 177 | 520305 | 4156228 | 1957 | 1183.38 | 135.89 | 132.87 | 96.15 | 109.47 | 109.61 |
| 178 | 520298 | 4156128 | 1955 | 1184.38 | 136.00 | 133.06 | 95.72 | 109.27 | 109.42 |
| 179 | 520282 | 4156020 | 1959 | 1183.20 | 135.86 | 133.00 | 96.90 | 110.00 | 110.11 |
| 180 | 520262 | 4155917 | 1960 | 1178.09 | 135.26 | 132.49 | 96.69 | 109.68 | 109.83 |
| 181 | 520241 | 4155813 | 1958 | 1177.08 | 135.14 | 132.45 | 96.03 | 109.24 | 109.50 |
| 182 | 520230 | 4155712 | 1957 | 1175.63 | 134.97 | 132.36 | 95.63 | 108.95 | 109.22 |
| 183 | 520239 | 4155601 | 1958 | 1173.25 | 134.69 | 132.16 | 95.75 | 108.96 | 109.11 |

| <i>stn</i> | <i>x</i> | <i>y</i> | <i>elev</i> | <i>field g</i> | <i>rel g</i> | <i>latitude</i> | <i>free air</i> | <i>bouguer</i> | <i>complete</i> |
|------------|----------|----------|-------------|----------------|--------------|-----------------|-----------------|----------------|-----------------|
| 184 | 520249 | 4155506 | 1962 | 1163.70 | 133.57 | 131.12 | 95.94 | 108.71 | 108.87 |
| 185 | 520254 | 4155408 | 1963 | 1163.16 | 133.51 | 131.13 | 96.26 | 108.91 | 109.05 |
| 186 | 520254 | 4155307 | 1965 | 1160.50 | 133.19 | 130.90 | 96.65 | 109.07 | 109.22 |
| 187 | 520219 | 4155210 | 1966 | 1154.95 | 132.55 | 130.33 | 96.38 | 108.70 | 108.85 |
| 188 | 520189 | 4155116 | 1967 | 1147.46 | 131.67 | 129.53 | 95.89 | 108.09 | 108.23 |
| 189 | 520155 | 4155016 | 1973 | 1144.47 | 131.32 | 129.26 | 97.47 | 109.00 | 109.16 |
| 190 | 520099 | 4154927 | 1975 | 1140.92 | 130.91 | 128.92 | 97.75 | 109.05 | 109.28 |
| 191 | 520051 | 4154835 | 1976 | 1138.35 | 130.61 | 128.69 | 97.83 | 109.03 | 109.20 |
| 192 | 520010 | 4154729 | 1977 | 1134.24 | 130.14 | 128.30 | 97.75 | 108.83 | 109.22 |
| 193 | 519970 | 4154629 | 1983 | 1125.51 | 129.13 | 127.37 | 98.67 | 109.08 | 109.41 |
| 194 | 519915 | 4154542 | 1982 | 1117.42 | 128.19 | 126.50 | 97.49 | 108.01 | 108.18 |
| 195 | 519869 | 4154451 | 1981 | 1117.73 | 128.22 | 126.60 | 97.29 | 107.92 | 108.12 |
| 196 | 519837 | 4154344 | 1978 | 1113.25 | 127.71 | 126.17 | 95.93 | 106.90 | 107.03 |
| 197 | 519789 | 4154250 | 1984 | 1102.36 | 126.44 | 124.98 | 96.59 | 106.89 | 107.57 |
| 198 | 519680 | 4154181 | 1995 | 1087.42 | 124.71 | 123.30 | 98.30 | 107.37 | 108.30 |
| 199 | 519583 | 4154135 | 1999 | 1078.03 | 123.62 | 122.25 | 98.49 | 107.11 | 113.51 |
| 200 | 521263 | 4154274 | 2051 | 993.31 | 113.78 | 112.30 | 104.58 | 107.38 | 114.61 |
| 201 | 521165 | 4154236 | 2056 | 986.35 | 112.97 | 111.52 | 105.35 | 107.59 | 114.49 |
| 202 | 521068 | 4154192 | 2057 | 992.82 | 113.72 | 112.31 | 106.45 | 108.57 | 114.81 |
| 203 | 520970 | 4154186 | 2051 | 997.29 | 114.25 | 112.84 | 105.12 | 107.92 | 113.81 |
| 204 | 520868 | 4154221 | 2047 | 1002.26 | 114.83 | 113.39 | 104.44 | 107.69 | 113.36 |
| 205 | 520771 | 4154265 | 2041 | 1008.17 | 115.52 | 114.04 | 103.24 | 107.16 | 112.40 |
| 206 | 520672 | 4154278 | 2040 | 1013.04 | 116.09 | 114.61 | 103.50 | 107.53 | 112.37 |
| 207 | 520597 | 4154224 | 2037 | 1027.73 | 117.80 | 116.36 | 104.33 | 108.69 | 114.80 |
| 208 | 521255 | 4154168 | 2050 | 997.08 | 114.24 | 112.85 | 104.82 | 107.73 | 113.76 |
| 209 | 521228 | 4154068 | 2051 | 989.42 | 113.35 | 112.04 | 104.32 | 107.12 | 112.86 |
| 210 | 521213 | 4153968 | 2050 | 988.68 | 113.27 | 112.03 | 104.01 | 106.92 | 112.75 |
| 211 | 521315 | 4153902 | 2052 | 982.91 | 112.60 | 111.42 | 104.01 | 106.70 | 113.15 |
| 212 | 521370 | 4153815 | 2056 | 974.67 | 111.65 | 110.53 | 104.36 | 106.60 | 112.96 |
| 213 | 521426 | 4153732 | 2060 | 968.86 | 110.98 | 109.92 | 104.99 | 106.78 | 113.30 |
| 214 | 521475 | 4153644 | 2063 | 960.80 | 110.04 | 109.06 | 105.05 | 106.51 | 113.63 |
| 215 | 521502 | 4153548 | 2070 | 952.16 | 109.04 | 108.14 | 106.28 | 106.96 | 114.12 |
| 216 | 521509 | 4153446 | 2072 | 945.26 | 108.24 | 107.42 | 106.18 | 106.63 | 114.68 |
| 217 | 521493 | 4153341 | 2082 | 934.35 | 106.98 | 106.23 | 108.09 | 107.41 | 115.41 |
| 218 | 521529 | 4153252 | 2083 | 924.88 | 105.85 | 105.18 | 107.34 | 106.55 | 114.75 |
| 219 | 521603 | 4153180 | 2086 | 919.33 | 105.20 | 104.58 | 107.67 | 106.55 | 115.25 |
| 220 | 521624 | 4153075 | 2089 | 917.42 | 104.98 | 104.44 | 108.46 | 107.00 | 114.93 |
| 221 | 521574 | 4152945 | 2084 | 923.30 | 105.66 | 105.23 | 107.69 | 106.80 | 114.37 |
| 222 | 521474 | 4152980 | 2087 | 928.51 | 106.26 | 105.80 | 109.20 | 107.96 | 115.40 |
| 223 | 521366 | 4152996 | 2082 | 938.42 | 107.41 | 106.94 | 108.79 | 108.12 | 114.82 |
| 224 | 521267 | 4152959 | 2076 | 946.51 | 108.35 | 107.90 | 107.90 | 107.90 | 113.85 |
| 225 | 521164 | 4152953 | 2069 | 953.65 | 109.18 | 108.74 | 106.58 | 107.36 | 113.35 |
| 226 | 521057 | 4153029 | 2068 | 956.43 | 109.50 | 109.01 | 106.54 | 107.43 | 113.35 |
| 227 | 520962 | 4153114 | 2066 | 961.26 | 110.07 | 109.50 | 106.42 | 107.54 | 113.74 |
| 228 | 520934 | 4153221 | 2067 | 967.67 | 110.82 | 110.17 | 107.39 | 108.40 | 114.54 |
| 229 | 520901 | 4153309 | 2065 | 972.72 | 111.41 | 110.69 | 107.29 | 108.52 | 114.05 |
| 230 | 520845 | 4153400 | 2061 | 969.83 | 111.07 | 110.28 | 105.66 | 107.33 | 112.53 |

| <i>stn</i> | <i>x</i> | <i>y</i> | <i>elev</i> | <i>field g</i> | <i>rel g</i> | <i>latitude</i> | <i>free air</i> | <i>bouguer</i> | <i>complete</i> |
|------------|----------|----------|-------------|----------------|--------------|-----------------|-----------------|----------------|-----------------|
| 231 | 520738 | 4153437 | 2054 | 970.36 | 111.14 | 110.32 | 103.53 | 105.99 | 110.42 |
| 232 | 520662 | 4153472 | 2046 | 994.13 | 113.91 | 113.06 | 103.80 | 107.16 | 110.02 |
| 233 | 520611 | 4153584 | 2029 | 1013.64 | 116.18 | 115.24 | 100.74 | 106.00 | 108.35 |
| 234 | 520518 | 4153643 | 2023 | 1026.25 | 117.65 | 116.66 | 100.31 | 106.24 | 108.76 |
| 235 | 520423 | 4153687 | 2024 | 1029.52 | 118.03 | 117.01 | 100.96 | 106.79 | 109.87 |
| 236 | 520270 | 4153718 | 2029 | 1018.45 | 116.75 | 115.70 | 101.20 | 106.46 | 110.30 |
| 237 | 520152 | 4153681 | 2037 | 1005.35 | 115.23 | 114.21 | 102.18 | 106.54 | 110.52 |
| 238 | 520116 | 4153638 | 2039 | 996.25 | 114.17 | 113.19 | 101.77 | 105.91 | 111.35 |
| 239 | 520831 | 4153150 | 2061 | 961.18 | 110.10 | 109.51 | 104.88 | 106.56 | 111.63 |
| 240 | 520722 | 4153115 | 2058 | 970.32 | 111.17 | 110.61 | 105.05 | 107.07 | 111.48 |
| 241 | 520606 | 4153102 | 2055 | 974.95 | 111.71 | 111.15 | 104.67 | 107.03 | 110.98 |
| 243 | 520398 | 4153147 | 2047 | 981.36 | 112.46 | 111.86 | 102.91 | 106.16 | 110.60 |
| 242 | 520504 | 4153127 | 2052 | 984.55 | 112.83 | 112.25 | 104.84 | 107.53 | 111.34 |
| 244 | 520311 | 4153182 | 2045 | 988.71 | 113.31 | 112.69 | 103.12 | 106.59 | 110.34 |
| 245 | 520198 | 4153212 | 2044 | 999.79 | 114.60 | 113.96 | 104.08 | 107.66 | 110.64 |
| 246 | 520061 | 4153176 | 2037 | 1009.75 | 115.76 | 115.14 | 103.11 | 107.47 | 115.08 |
| 247 | 521608 | 4152825 | 2083 | 925.98 | 106.02 | 105.68 | 107.84 | 107.06 | 113.59 |
| 248 | 521660 | 4152733 | 2078 | 927.94 | 106.25 | 105.98 | 106.60 | 106.38 | 112.53 |
| 249 | 521709 | 4152635 | 2076 | 919.02 | 105.21 | 105.02 | 105.02 | 105.02 | 111.16 |
| 250 | 521771 | 4152517 | 2078 | 916.44 | 104.91 | 104.82 | 105.44 | 105.21 | 111.49 |
| 251 | 521803 | 4152422 | 2081 | 914.83 | 104.73 | 104.71 | 106.25 | 105.69 | 112.16 |
| 252 | 521845 | 4152304 | 2085 | 909.61 | 104.12 | 104.19 | 106.97 | 105.96 | 112.65 |
| 253 | 521876 | 4152201 | 2089 | 903.87 | 103.45 | 103.61 | 107.62 | 106.16 | 112.85 |
| 254 | 521887 | 4152145 | 2090 | 903.17 | 103.37 | 103.57 | 107.89 | 106.32 | 112.82 |
| 255 | 521782 | 4152102 | 2089 | 900.20 | 103.02 | 103.26 | 107.27 | 105.81 | 112.49 |
| 256 | 521658 | 4152087 | 2091 | 889.13 | 101.74 | 101.98 | 106.61 | 104.93 | 111.98 |
| 257 | 521575 | 4152059 | 2095 | 886.72 | 101.46 | 101.72 | 107.59 | 105.46 | 112.38 |
| 258 | 521473 | 4151998 | 2095 | 887.16 | 101.51 | 101.82 | 107.69 | 105.56 | 111.72 |
| 259 | 521360 | 4151955 | 2092 | 887.76 | 101.58 | 101.93 | 106.86 | 105.07 | 111.90 |
| 260 | 521381 | 4151844 | 2097 | 879.73 | 100.64 | 101.08 | 107.56 | 105.21 | 112.04 |
| 261 | 521357 | 4151739 | 2099 | 882.13 | 100.92 | 101.44 | 108.54 | 105.96 | 112.47 |
| 262 | 521378 | 4151639 | 2098 | 879.12 | 100.57 | 101.17 | 107.96 | 105.50 | 111.90 |
| 263 | 521413 | 4151506 | 2103 | 867.50 | 99.22 | 99.92 | 108.26 | 105.23 | 112.26 |
| 264 | 521461 | 4151373 | 2108 | 853.25 | 97.56 | 98.37 | 108.25 | 104.66 | 111.22 |
| 265 | 521594 | 4151327 | 2108 | 848.01 | 96.96 | 97.80 | 107.67 | 104.09 | 109.78 |
| 266 | 522403 | 4152396 | 2076 | 927.71 | 106.14 | 106.14 | 106.14 | 106.14 | 112.18 |
| 267 | 522312 | 4152355 | 2080 | 918.91 | 105.11 | 105.15 | 106.38 | 105.93 | 112.23 |
| 268 | 522215 | 4152327 | 2083 | 911.05 | 104.19 | 104.25 | 106.41 | 105.62 | 112.03 |
| 269 | 522131 | 4152268 | 2085 | 902.44 | 103.18 | 103.29 | 106.06 | 105.06 | 111.85 |
| 270 | 522035 | 4152197 | 2090 | 896.00 | 102.42 | 102.58 | 106.90 | 105.34 | 111.54 |
| 271 | 521957 | 4152134 | 2089 | 902.11 | 103.13 | 103.34 | 107.35 | 105.89 | 111.60 |
| 272 | 521902 | 4152025 | 2083 | 907.54 | 103.75 | 104.05 | 106.21 | 105.42 | 110.05 |
| 273 | 521921 | 4151923 | 2078 | 913.85 | 104.48 | 104.86 | 105.47 | 105.25 | 109.50 |
| 274 | 521908 | 4151831 | 2073 | 924.21 | 105.68 | 106.13 | 105.20 | 105.54 | 109.86 |
| 275 | 521933 | 4151711 | 2076 | 919.71 | 105.15 | 105.69 | 105.69 | 105.69 | 109.99 |
| 276 | 522041 | 4151654 | 2080 | 908.58 | 103.85 | 104.44 | 105.67 | 105.22 | 110.58 |
| 277 | 522152 | 4151593 | 2088 | 896.64 | 102.46 | 103.09 | 106.79 | 105.45 | 110.76 |

| <i>stn</i> | <i>x</i> | <i>y</i> | <i>elev</i> | <i>field g</i> | <i>rel g</i> | <i>latitude</i> | <i>free air</i> | <i>bouguer</i> | <i>complete</i> |
|------------|----------|----------|-------------|----------------|--------------|-----------------|-----------------|----------------|-----------------|
| 278 | 522265 | 4151567 | 2088 | 889.57 | 101.63 | 102.28 | 105.99 | 104.64 | 109.78 |
| 279 | 522353 | 4151625 | 2082 | 903.83 | 103.28 | 103.89 | 105.74 | 105.07 | 109.98 |
| 280 | 522456 | 4151684 | 2082 | 908.12 | 103.77 | 104.33 | 106.18 | 105.51 | 110.01 |
| 281 | 522527 | 4151738 | 2080 | 912.15 | 104.23 | 104.75 | 105.98 | 105.54 | 110.38 |
| 282 | 522634 | 4151753 | 2080 | 913.62 | 104.39 | 104.90 | 106.14 | 105.69 | 110.15 |
| 283 | 522727 | 4151767 | 2076 | 909.12 | 103.86 | 104.36 | 104.36 | 104.36 | 108.20 |
| 284 | 522805 | 4151826 | 2069 | 929.72 | 106.23 | 106.68 | 104.52 | 105.31 | 108.91 |
| 285 | 522896 | 4151869 | 2066 | 934.81 | 106.81 | 107.23 | 104.15 | 105.27 | 108.59 |
| 286 | 523001 | 4151893 | 2066 | 937.26 | 107.09 | 107.49 | 104.41 | 105.52 | 108.76 |
| 287 | 523101 | 4151891 | 2062 | 941.31 | 107.56 | 107.96 | 103.64 | 105.21 | 108.15 |
| 288 | 523198 | 4151901 | 2059 | 947.27 | 108.24 | 108.63 | 103.39 | 105.29 | 107.72 |
| 289 | 523298 | 4151894 | 2054 | 956.18 | 109.26 | 109.66 | 102.87 | 105.33 | 106.98 |
| 290 | 523371 | 4151833 | 2047 | 971.25 | 110.96 | 111.40 | 102.45 | 105.70 | 106.48 |
| 292 | 523468 | 4151685 | 2027 | 997.39 | 113.95 | 114.45 | 99.33 | 104.82 | 105.00 |
| 293 | 523495 | 4151604 | 2021 | 1011.88 | 115.63 | 116.19 | 99.22 | 105.37 | 105.87 |
| 294 | 523481 | 4151538 | 2017 | 1024.49 | 117.07 | 117.70 | 99.50 | 106.10 | 106.98 |
| 295 | 523460 | 4151388 | 1999 | 1046.83 | 119.66 | 120.34 | 96.58 | 105.20 | 107.99 |
| 296 | 523522 | 4151308 | 2013 | 1027.04 | 117.35 | 118.15 | 98.70 | 105.76 | 107.34 |
| 297 | 523573 | 4151229 | 2024 | 1015.39 | 115.98 | 116.84 | 100.79 | 106.61 | 107.39 |
| 298 | 523669 | 4151198 | 2030 | 999.00 | 114.06 | 114.98 | 100.79 | 105.94 | 106.35 |
| 299 | 523756 | 4151143 | 2032 | 982.25 | 112.10 | 113.05 | 99.47 | 104.40 | 104.66 |
| 300 | 523819 | 4151069 | 2033 | 981.21 | 111.96 | 112.95 | 99.68 | 104.50 | 104.89 |
| 301 | 523881 | 4150993 | 2033 | 984.63 | 112.36 | 113.41 | 100.14 | 104.95 | 105.42 |
| 302 | 523937 | 4150908 | 2028 | 993.68 | 113.40 | 114.51 | 99.70 | 105.08 | 105.82 |
| 303 | 523955 | 4150810 | 2037 | 974.15 | 111.13 | 112.31 | 100.27 | 104.64 | 105.09 |
| 304 | 523943 | 4150690 | 2041 | 956.62 | 109.09 | 110.34 | 99.54 | 103.46 | 103.81 |
| 305 | 523996 | 4150603 | 2039 | 966.16 | 110.20 | 111.54 | 100.13 | 104.27 | 104.69 |
| 306 | 524086 | 4150574 | 2036 | 974.84 | 111.20 | 112.62 | 100.28 | 104.75 | 105.39 |
| 307 | 524149 | 4150497 | 2031 | 984.95 | 112.37 | 113.82 | 99.93 | 104.97 | 106.33 |
| 308 | 524208 | 4150412 | 2024 | 991.71 | 113.16 | 114.66 | 98.61 | 104.43 | 106.58 |
| 309 | 524294 | 4150362 | 2015 | 1000.61 | 114.19 | 115.76 | 96.93 | 103.76 | 106.61 |
| 310 | 524396 | 4150348 | 2008 | 1018.43 | 116.26 | 117.86 | 96.88 | 104.49 | 108.41 |
| 311 | 524499 | 4150333 | 2004 | 1032.96 | 117.94 | 119.56 | 97.34 | 105.40 | 109.77 |
| 312 | 524590 | 4150298 | 1994 | 1044.88 | 119.33 | 120.96 | 95.65 | 104.83 | 110.32 |
| 313 | 524583 | 4150176 | 1986 | 1060.26 | 121.11 | 122.77 | 95.00 | 105.07 | 111.66 |
| 314 | 523407 | 4151952 | 2047 | 968.69 | 110.41 | 112.17 | 103.22 | 106.47 | 108.32 |
| 315 | 523489 | 4152009 | 2047 | 977.04 | 111.38 | 111.73 | 102.79 | 106.03 | 108.00 |
| 316 | 523564 | 4152078 | 2053 | 973.13 | 110.92 | 111.23 | 104.13 | 106.71 | 109.39 |
| 317 | 523644 | 4152143 | 2060 | 961.10 | 109.51 | 109.77 | 104.83 | 106.62 | 110.14 |
| 318 | 523726 | 4152200 | 2064 | 952.55 | 108.51 | 108.72 | 105.01 | 106.36 | 110.07 |
| 319 | 523828 | 4152204 | 2061 | 953.21 | 108.59 | 108.74 | 104.12 | 105.80 | 109.53 |
| 320 | 523932 | 4152225 | 2055 | 966.34 | 110.11 | 110.27 | 103.78 | 106.14 | 108.98 |
| 321 | 523954 | 4152323 | 2048 | 990.20 | 112.88 | 113.02 | 104.38 | 107.51 | 110.14 |
| 322 | 524016 | 4152427 | 2051 | 992.60 | 113.15 | 113.21 | 105.50 | 108.30 | 111.43 |
| 323 | 523919 | 4152118 | 2050 | 972.88 | 110.85 | 110.83 | 102.81 | 105.72 | 108.17 |
| 324 | 523900 | 4152019 | 2044 | 984.78 | 112.23 | 112.45 | 102.58 | 106.16 | 107.86 |
| 325 | 523960 | 4151936 | 2036 | 993.15 | 113.20 | 113.50 | 101.16 | 105.63 | 106.50 |

| <i>stn</i> | <i>x</i> | <i>y</i> | <i>elev</i> | <i>field g</i> | <i>rel g</i> | <i>latitude</i> | <i>free air</i> | <i>bouguer</i> | <i>complete</i> |
|------------|----------|----------|-------------|----------------|--------------|-----------------|-----------------|----------------|-----------------|
| 326 | 524011 | 4151855 | 2036 | 995.42 | 113.46 | 113.83 | 101.48 | 105.96 | 106.71 |
| 327 | 524100 | 4151789 | 2029 | 1003.51 | 114.39 | 114.82 | 100.32 | 105.58 | 105.79 |
| 328 | 524155 | 4151704 | 2018 | 1013.26 | 115.52 | 116.01 | 98.11 | 104.60 | 105.16 |
| 340 | 524053 | 4150698 | 2037 | 969.92 | 110.63 | 111.18 | 99.15 | 103.51 | 103.94 |
| 341 | 524156 | 4150691 | 2038 | 968.37 | 110.46 | 111.80 | 100.08 | 104.33 | 104.85 |
| 342 | 524255 | 4150693 | 2038 | 966.39 | 110.24 | 111.59 | 99.86 | 104.12 | 104.63 |
| 343 | 524358 | 4150701 | 2031 | 967.63 | 110.40 | 111.75 | 97.86 | 102.90 | 103.92 |
| 344 | 524457 | 4150732 | 2032 | 979.52 | 111.79 | 113.13 | 99.55 | 104.48 | 105.37 |
| 345 | 523784 | 4150520 | 2046 | 951.51 | 108.52 | 109.83 | 100.57 | 103.93 | 104.14 |
| 346 | 523691 | 4150471 | 2049 | 947.05 | 107.98 | 109.47 | 101.14 | 104.16 | 104.35 |
| 347 | 523595 | 4150473 | 2053 | 944.15 | 107.64 | 109.16 | 102.06 | 104.64 | 104.84 |
| 348 | 523489 | 4150480 | 2055 | 940.95 | 107.26 | 108.78 | 102.30 | 104.65 | 104.93 |
| 349 | 523379 | 4150568 | 2063 | 928.59 | 105.81 | 107.33 | 103.31 | 104.77 | 105.67 |
| 350 | 523300 | 4150631 | 2060 | 932.66 | 106.28 | 107.72 | 102.78 | 104.57 | 105.34 |
| 351 | 523194 | 4150640 | 2059 | 934.08 | 106.43 | 107.83 | 102.58 | 104.48 | 105.18 |
| 352 | 523042 | 4150676 | 2058 | 934.91 | 106.52 | 107.91 | 102.35 | 104.37 | 105.04 |
| 353 | 522953 | 4150678 | 2060 | 928.87 | 105.81 | 107.17 | 102.23 | 104.02 | 104.85 |
| 354 | 522832 | 4150676 | 2069 | 909.68 | 103.57 | 104.92 | 102.76 | 103.55 | 105.15 |
| 355 | 522680 | 4150677 | 2079 | 899.66 | 102.39 | 103.75 | 104.68 | 104.34 | 106.91 |
| 356 | 522607 | 4150618 | 2082 | 896.62 | 102.03 | 103.38 | 105.24 | 104.56 | 107.32 |
| 357 | 522546 | 4150522 | 2087 | 887.39 | 100.95 | 102.35 | 105.74 | 104.51 | 107.60 |
| 358 | 522454 | 4150459 | 2093 | 873.02 | 99.27 | 100.75 | 105.99 | 104.09 | 107.68 |
| 359 | 522329 | 4150430 | 2096 | 863.89 | 98.19 | 99.72 | 105.89 | 103.66 | 107.51 |
| 360 | 522223 | 4150436 | 2097 | 859.44 | 97.81 | 99.36 | 105.84 | 103.49 | 107.44 |
| 361 | 522122 | 4150461 | 2099 | 858.08 | 97.65 | 99.19 | 106.29 | 103.72 | 107.94 |
| 362 | 522043 | 4150522 | 2100 | 857.04 | 97.53 | 99.05 | 106.46 | 103.77 | 107.92 |
| 363 | 522088 | 4150678 | 2089 | 878.18 | 99.99 | 101.46 | 105.47 | 104.02 | 107.60 |
| 364 | 522164 | 4150752 | 2083 | 886.07 | 100.90 | 102.26 | 104.42 | 103.63 | 106.44 |
| 365 | 522183 | 4150854 | 2078 | 892.81 | 101.69 | 102.98 | 103.60 | 103.38 | 106.18 |
| 366 | 522236 | 4150937 | 2075 | 900.14 | 102.54 | 103.76 | 103.45 | 103.56 | 106.22 |
| 367 | 522320 | 4150991 | 2072 | 908.67 | 103.53 | 104.68 | 103.45 | 103.90 | 106.35 |
| 368 | 522417 | 4151032 | 2064 | 919.72 | 104.82 | 105.92 | 102.22 | 103.56 | 105.31 |

Appendix C

USGS Report FS-239-95

Introduction to Potential Fields: Gravity